

NASA CR - 135019



DOUBLE ION PRODUCTION IN MERCURY THRUSTERS

(NASA-CR-135019) DOUBLE ION PRODUCTION IN
MERCURY THRUSTERS M.S. Thesis (Colorado
State Univ.) 86 p HC \$5.00 CSCL 21C

N76-22299

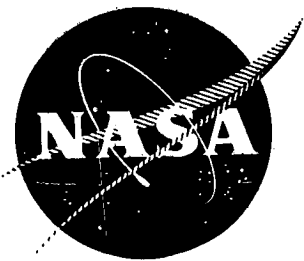
Unclass
G3/20 26906

PREPARED FOR
LEWIS RESEARCH CENTER
NATIONAL AERONAUTICS AND SPACE ADMINISTRATION
Grant NGR-06-002-112

by
Ralph R. Peters

Approved by
Paul J. Wilbur
April 1976
Department of Mechanical Engineering
Colorado State University
Fort Collins, Colorado





DOUBLE ION PRODUCTION IN MERCURY THRUSTERS

PREPARED FOR
LEWIS RESEARCH CENTER
NATIONAL AERONAUTICS AND SPACE ADMINISTRATION
Grant NGR-06-002-112

by
Ralph R. Peters

Approved by
Paul J. Wilbur
April 1976
Department of Mechanical Engineering
Colorado State University
Fort Collins, Colorado

1. Report No. NASA CR - 135019	2. Government Accession No.	3. Recipient's Catalog No	
4. Title and Subtitle DOUBLE ION PRODUCTION IN MERCURY THRUSTERS		5. Report Date May, 1976	
		6. Performing Organization Code	
7. Author(s) Ralph R. Peters and Paul J. Wilbur		8. Performing Organization Report No.	
		10. Work Unit No.	
9. Performing Organization Name and Address Department of Mechanical Engineering Colorado State University Fort Collins, Colorado 80523		11. Contract or Grant No. NGR-06-002-i12	
		13. Type of Report and Period Covered	
12. Sponsoring Agency Name and Address National Aeronautics and Space Administration Washington, D. C. 20546		14. Sponsoring Agency Code	
15. Supplementary Notes Grant Monitor - William Kerslake, NASA Lewis Research Center, Cleveland, Ohio 44135. This report is a reproduction of the M.S. Thesis of Mr. Ralph R. Peters. It is submitted to the sponsor and to the distribution list in this form both as a presentation of the technical material, and as an indication of the academic program supported by this Grant.			
16. Abstract Significant densities of doubly charged ions exist in the discharge chambers of electron bombardment ion thrusters. These ions are undesirable because they are a major plasma constituent effecting the sputtering damage which limits thruster lifetime. It would be desirable to reduce their density while maintaining good thruster performance. The development of a model which predicts the doubly charged ion density is discussed. The accuracy of the model is shown to be good for two different thruster sizes and a total of 11 different cases. The model indicates that in most cases more than 80% of the doubly charged ions are produced from singly charged ions. This result can be used to develop a much simpler model which, along with correlations of the average plasma properties, can be used to determine the doubly charged ion density in ion thrusters with acceptable accuracy. Two different techniques which can be used to reduce the doubly charged ion density, while maintaining good thruster operation, are identified as a result of an examination of the simple model. First, the electron density can be reduced and the thruster size then increased to maintain the same propellant utilization. Second, at a fixed thruster size, the plasma density, temperature and energy can be reduced and then to maintain a constant propellant utilization the open area of the grids to neutral propellant loss can be reduced through the use of a small hole accelerator grid. The reduction in the values of the plasma properties causes a decrease in the doubly charged ion density.			
17. Key Words (Suggested by Author(s)) Electrostatic Thruster Mercury Discharge Chamber Model		18. Distribution Statement Unclassified - Unlimited	
19. Security Classif. (of this report) Unclassified	20. Security Classif. (of this page) Unclassified	21. No. of Pages 35	22. Price*

* For sale by the National Technical Information Service, Springfield, Virginia 22161

TABLE OF CONTENTS

	<u>Page</u>
ABSTRACT	i
TABLE OF CONTENTS	ii
LIST OF TABLES	iii
LIST OF FIGURES	iii
INTRODUCTION	1
THRUSTER OPERATION	2
THEORETICAL MODEL	6
Introduction	6
Electron Bombardment Reactions	10
Migration Losses	16
Photon Diffusion Losses	19
Determination of Specie Densities	21
EXPERIMENTAL PROCEDURES AND RESULTS	24
RESULTS AND DISCUSSION	32
SIMPLIFIED MODEL	39
CONCLUSIONS	55
REFERENCES	56
APPENDIX A: Listing of the Computer Program HG	58
APPENDIX B: Listing of the Computer Program PROP	73

LIST OF TABLES

<u>Table Number</u>		<u>Page</u>
I Thruster Sizes, Configurations and Conditions	26	
II Experimental Results	29	
III Predicted Densities and Reaction Rates	36	
IV Determination of the Double Ion Density Using the Simplified Model	51	

LIST OF FIGURES

<u>Figure Number</u>		<u>Page</u>
1 Electron Bombardment Ion Thruster Schematic	3	
2 Discharge Chamber Reaction Schematic	7	
3 Mercury Cross Sections	12	
4 Plasma Property Profiles, 15 cm Thruster - SERT II Grids - 37 V Anode Voltage	28	
5 Double-to-Single Ion Density Ratio in a 15 cm Diameter Thruster	33	
6 Double-to-Single Ion Density Ratio in a 30 cm Diameter Thruster	34	
7 Rate Factors for $Hg^+ \rightarrow Hg^{++}$	41	
8 Maxwellian Electron Temperature Correlation	43	
9 Primary Electron Energy Correlation	45	
10 Electron Density Correlation	47	
11 Primary Electron Density Correlation	48	
12 Uniformity Factor Correlation	49	

INTRODUCTION

Electron bombardment ion thrusters are presently being considered for use in deep space probes and for satellite stationkeeping functions. These devices which have the advantage of very high specific impulses also have the attendant disadvantage of low thrust densities. This low thrust characteristic necessitates thruster operation for long periods of time in order to accomplish typical missions (of the order of 10,000 hours). Thruster lifetimes can be limited by the erosion of ion chamber component parts with most of this erosion (or sputtering damage) being caused by doubly charged ions. Long thruster lifetimes therefore require control of doubly charged ion densities.

Many experiments could be performed to determine how the thruster should be operated so that thruster performance would be good and the doubly charged ion density would be reduced to an acceptable level. However, these experiments would have the disadvantage of being time consuming and costly and the results might be applicable to one size and type of thruster only. Instead a theoretical model could be developed which would accurately predict the doubly charged ion density over a wide range of conditions and thruster sizes. This model could be applied at low cost to determine the factors affecting the doubly charged ion density and how they should be adjusted to reduce the double ion density. It should also indicate what effects these changes would have on thruster performance. Such a model has been developed for electron bombardment ion thrusters and has been verified experimentally for thrusters which use mercury propellant. A discussion of the model's development and verification is presented in this paper along with some results and conclusions based upon the model.

THRUSTER OPERATION

Many of the assumptions and approximations used in the development of the model are based upon a knowledge of thruster operation. This section will briefly discuss thruster operation so that the development of the model in the next section will be more easily understood.

An ion thruster has two basic tasks to perform:

- 1) Ionization of the neutral propellant atoms.
- 2) Acceleration of the ions to high velocities producing thrust.

These two topics will form the basis for the discussion of thruster operation.

Figure 1 shows a schematic for a typical electron bombardment ion thruster. The specific type shown has a strongly divergent magnetic field which is presently the most common type. However, the operation of all types of electron bombardment ion thrusters is very similar⁽¹⁾. Electrons are emitted from the cathode and are drawn toward the anode which is biased 30-40V positive with respect to the cathode. These electrons (called primary electrons) are injected into the primary electron region with an energy slightly less than that associated with the 30-40V anode voltage. Electrons in this region are kept from going immediately to the anode by a magnetic field set up between the cathode pole piece and the anode pole piece but collisions eventually facilitate electron diffusion across these magnetic field lines so that they can be collected by the anode. As a result of the magnetic field containment the electron density is much higher ($\sim 10^{11} \text{ cm}^{-3}$) within this region than it is outside of it. The primary electron region's boundary is defined by the surface of revolution of the critical (magnetic) field line and the screen grid. Because the strength of the magnetic field

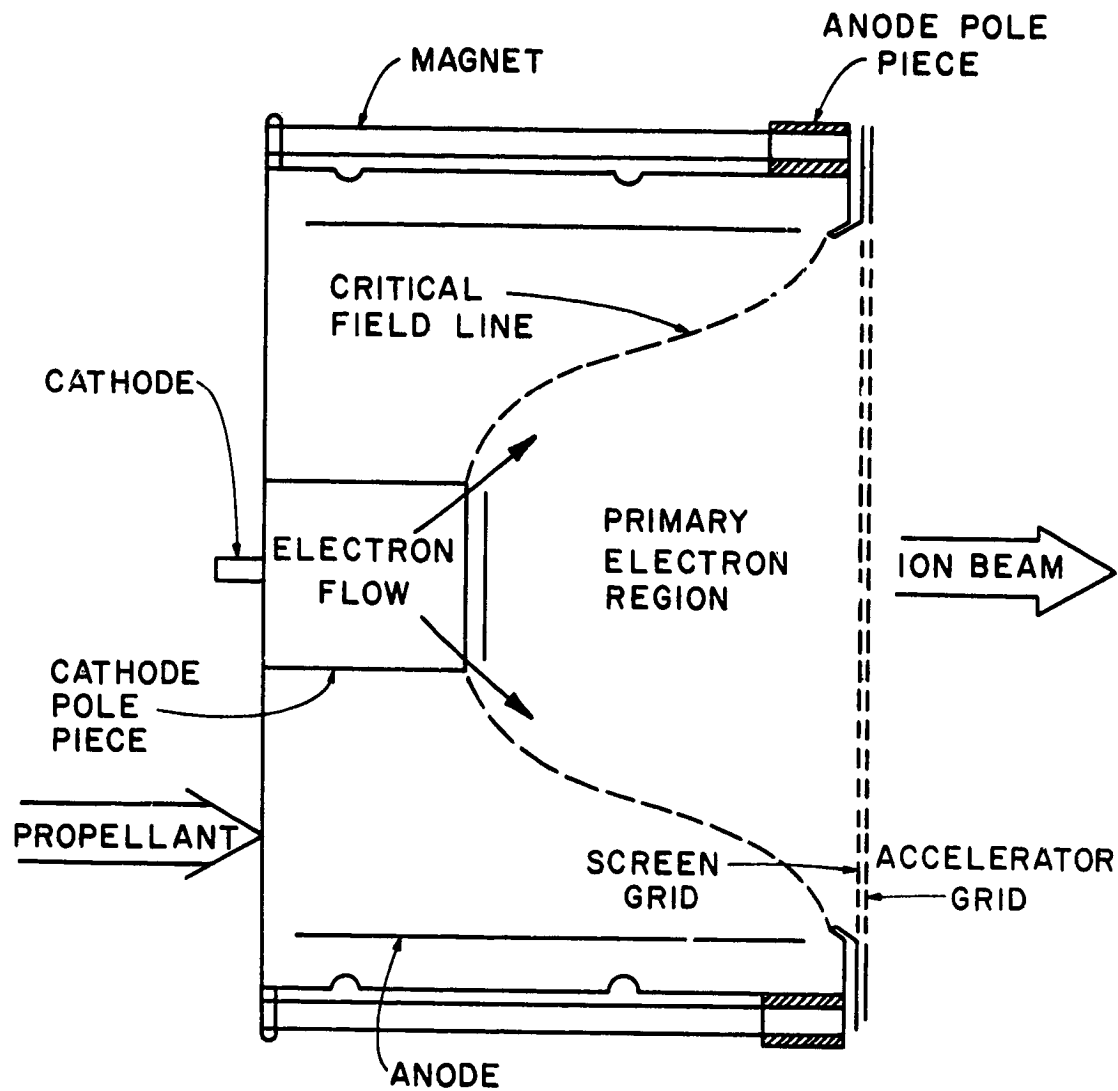


Figure 1 Electron Bombardment Ion Thruster Schematic

is fairly low within it, a fairly uniform electron density exists throughout the entire region.

Neutral propellant (e.g. mercury) is injected into the upstream end of the discharge chamber at low pressure (10^{-4} torr). Most of the interactions between electrons and neutral propellant atoms take place in the primary electron region because higher electron densities and energies exist there. Electrons bombard the neutral atoms occasionally knocking an outer shell electron loose from the atom forming a singly charged ion. The production of a mercury single ion requires more than 10 eV of energy from the incident electron. This electron and the ejected electron then share the remainder of the energy which the incident electron carried originally. This reaction results in the replacement of one high energy electron with two lower energy electrons which rapidly randomize with similarly generated electrons to form a Maxwellian electron group. Ions are extracted from the plasma through holes in the screen and accelerator grids as a result of the large potential difference applied across these two grids. The rate of ion loss through the grids times the ionic charge is called the beam current.

Electron bombardment of atoms and ions also produces doubly charged ions. Many of these ions are extracted from the discharge chamber by the grids, however, some of them go to the walls. As ions near the walls (the cathode pole piece, screen grid, etc.) they are accelerated to high velocities by an electric field that exists at the plasma boundary. When these high velocity ions strike the walls they can knock atoms loose (sputter atoms) from the walls of the discharge chamber. The energy that doubly charged ions possess upon striking the

walls is twice that of singly charged ions, therefore the sputtering damage caused by a double ion is much greater than that caused by a single ion. Double ions are thought to cause most of the sputtering damage even though their density is typically an order of magnitude less than that of the single ions.

THEORETICAL MODEL

Introduction

In order to develop a simple model for determining the double ion density in the discharge chamber only those ionic and atomic species which were considered significant in determining the double ion density were included. The significant species were selected as those which have substantial electron impact cross sections of formation over the electron energy range of interest so that large numbers of these excited atoms or ions will be produced. These states also have sufficiently long effective lifetimes so that they can participate in production processes before they decay. Only those reactions which lead directly or indirectly to the production of double ions were included.

Figure 2 is a discharge chamber reaction schematic showing these dominant species and the reactions in which each specie can participate. The model has been developed for thrusters using mercury propellant but the general procedure is valid for thrusters using other propellants.

The symbols used in Figure 2 represent the following species:

Hg^0 - neutral ground state mercury

Hg^m - metastable neutral mercury (6^3P_0 and 6^3P_2 states)

Hg^r - resonance state neutral mercury (6^3P_1 and 6^1P_1 states)

Hg^+ - singly ionized ground state mercury

Hg^{m+} - singly ionized metastable mercury ($6^2D_{3/2}$ and $6^2D_{5/2}$ states)

Hg^{++} - doubly ionized ground state mercury

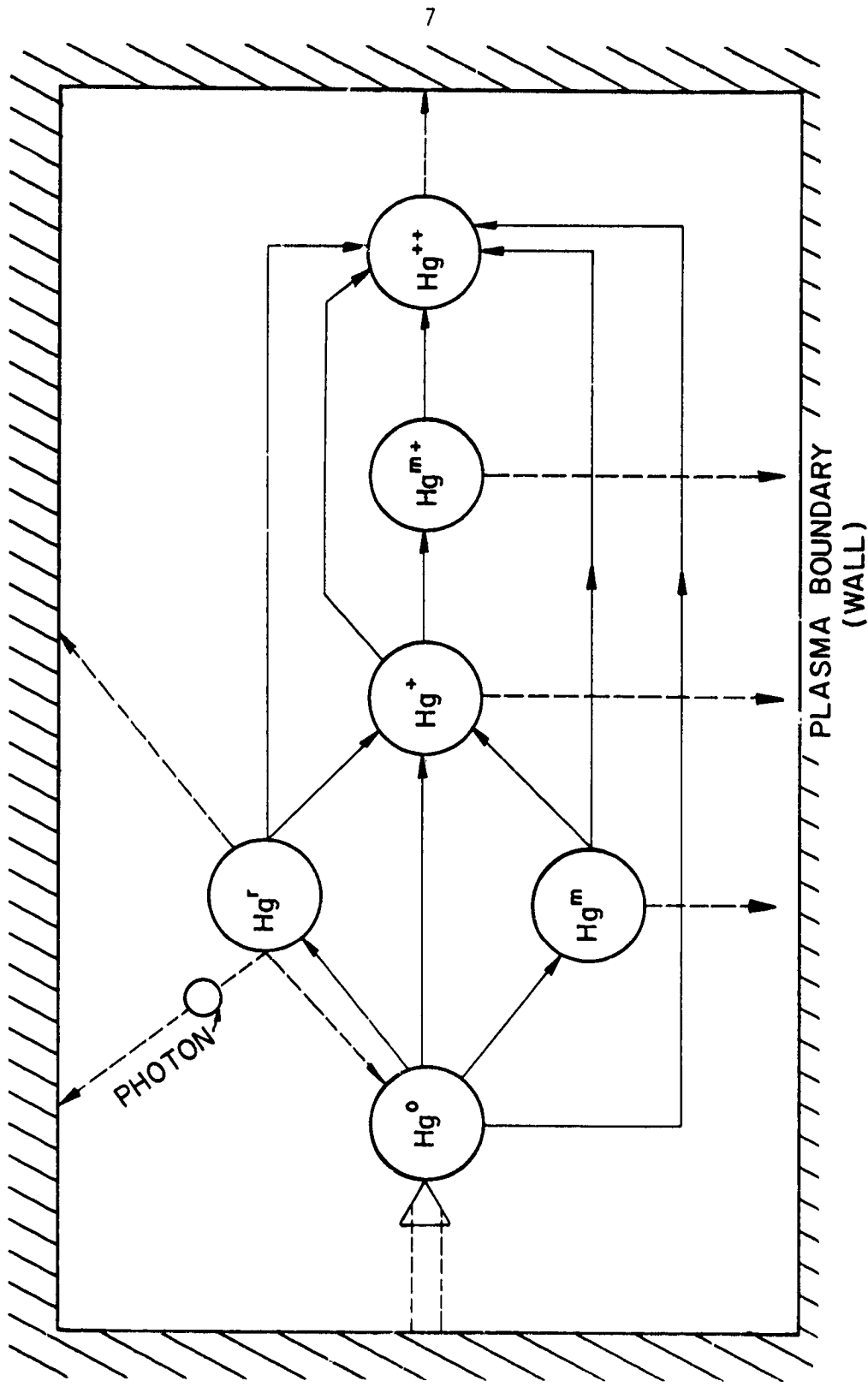


Figure 2 Discharge Chamber Reaction Schematic

The arrows in Figure 2 indicate the various interaction routes considered in this analysis. Three different types of reactions are indicated in this figure. The first type of reaction occurs when an electron interacts with an atom or ion producing a more highly excited specie. This reaction is indicated in Figure 2 by an arrow going from one specie to another more highly excited specie (e.g. the production of double ions from single ions). The production of a highly excited specie also represents a loss mechanism for the less excited specie. The reverse reaction in which, for example, an ion captures an electron is improbable because the reaction requires three bodies to simultaneously collide.

The second type of process is that of an atom or ion going to a plasma boundary. Such a boundary could be either the discharge chamber wall on which the atom or ion would be de-excited or it could be a grid aperture in which case the atom or ion would be extracted from the discharge region. In either case this represents a loss rate for any of the excited states. These losses to the boundary are indicated in Figure 2 by the dotted lines to the wall of the chamber. The large arrow back to the neutral ground state represents the resupply of neutral ground state atoms either from the walls or from the propellant supply system.

A third type of reaction shown in Figure 2 is relevant only to the two resonance states. The resonance states differ from metastable states in that they have a very short lifetime before they de-excite spontaneously by emitting a photon of light. However, the energy of this photon is such that it is readily absorbed by a nearby neutral ground state atom producing another resonance state atom. Since the

transport time of the photon is small compared to the excited state lifetime the excited state can be considered to exist continuously. Eventually the photon can diffuse to a boundary where it will be lost; this is equivalent to the loss of a resonance state atom. This loss mechanism is represented in Figure 2 by a dotted line conveying a photon to the wall and a branching line going from the resonance atom to the neutral ground state atom.

Figure 2 also shows the dominant routes for the production and loss of all of the excited atoms and ions considered. For example, ground state single ions can be produced as a result of electron bombardment of neutral-ground-state, resonance state, and metastable state atoms and these single ions can be lost as a result of single ion migration to the plasma boundary and the production of metastable single ions and double ions by electron bombardment.

When equilibrium conditions exist in the discharge chamber the rate of production of each specie must equal its loss rate. If, for example, the production rate of single ions increases, the single ion density must also increase to keep the loss rate (which is directly proportional to the single ion density) equal to the higher production rate. This example illustrates the fact that the equilibrium density of any specie is determined by the associated production and loss rates. If equations determining the production and loss rates could be derived, these equations could then be solved for the equilibrium density of any specie under consideration. The remainder of this section is concerned with deriving equations for the production and loss mechanisms indicated in Figure 2 and then solving these equations for the equilibrium densities of the various states.

Electron Bombardment Reactions

The first reaction to be considered is the one which produces excited atoms or ions by electron bombardment from less excited atoms or ions. The total rate of production of any specie γ from specie α (and hence the loss rate of α due to this reaction) is given by:

$$R_{\alpha}^{\gamma} = \int_{\text{Plasma Volume}} \int_{E=0}^{E=\infty} n_{\alpha} \sigma_{\alpha}^{\gamma}(E) v_e(E) dn_e dV \quad (1)$$

where n_{α} is the density of specie α at some point \vec{r} in the plasma, $\sigma_{\alpha}^{\gamma}(E)$ is the cross section for the production of γ from α at the electron energy $E^{(2-6)}$, v_e is the electron velocity at energy E , dn_e is the density of electrons with energies between E and $E + dE$ at \vec{r} , and dV is the infinitesimal volume element. The distribution of electrons over the energy spectrum of an ion thruster was assumed to be composed of a Maxwellian electron group which is described by a temperature (T_{mx} -- eV) and a density (n_{mx} -- cm^{-3}) and a monoenergetic group (primary electrons) which is described by an energy (ε_{pr} -- eV) and a density (n_{pr} -- cm^{-3}). This type of electron distribution is generally accepted as appropriate for electron bombardment thruster plasmas.^(1,7)

Substituting this electron distribution into Equation (1) and combining terms to form new functions results in the following equation.

$$R_{\alpha}^{\gamma} = \int_{\text{Volume}} n_{\alpha} [n_{pr} P_{\alpha}^{\gamma}(\varepsilon_{pr}) + n_{mx} Q_{\alpha}^{\gamma}(T_{mx})] dV \quad (2)$$

where

$$P_{\alpha}^{\gamma}(\varepsilon_{pr}) = v_e(\varepsilon_{pr}) \sigma_{\alpha}^{\gamma}(\varepsilon_{pr}) \quad (3)$$

and

$$Q_{\alpha}^Y(T_{mx}) = \int_{E=0}^{E=\infty} \sigma_{\alpha}^Y(E) v_e(E) \frac{dn_{mx}(E)}{n_{mx}} . \quad (4)$$

" $[dn_{mx}(E)/n_{mx}]$ " is the Maxwellian distribution function and the other terms are as defined previously.

Where possible the cross sections (σ_{α}^Y) required for Equations (3) and (4) were selected from experimental data.^(2,3,4) If experimental data were not available, theoretical cross sections were either obtained from the literature⁽⁵⁾ or calculated using the Gryzinski approximation.⁽⁶⁾ The Gryzinski approximation was modified for the cases of the metastable single ion production cross sections to reflect the significant value of the cross sections near the threshold. The cross sections used are presented in Figure 3 along with references indicating their origin.

Using integral equations like Equation (2) in the model would be inconvenient because it would then be very difficult to solve for the density of specie α (n_{α}) since n_{α} appears within the integral. For this reason it would be desirable to convert Equation (2) into a simple algebraic equation. Fortunately the plasma is fairly uniform in the primary electron region which is where most of the reactions take place. This suggests using average properties in Equation (2) to obtain the following result.

$$R_{\alpha}^Y = n_{\alpha}^* [n_{pr}^* p_{\alpha}^*(v_{pr}^*) + n_{mx}^* Q_{\alpha}^Y(T_{mx}^*)] V \quad (5)$$

The asterisks indicate volume averaged quantities and V is the volume of the primary electron region.

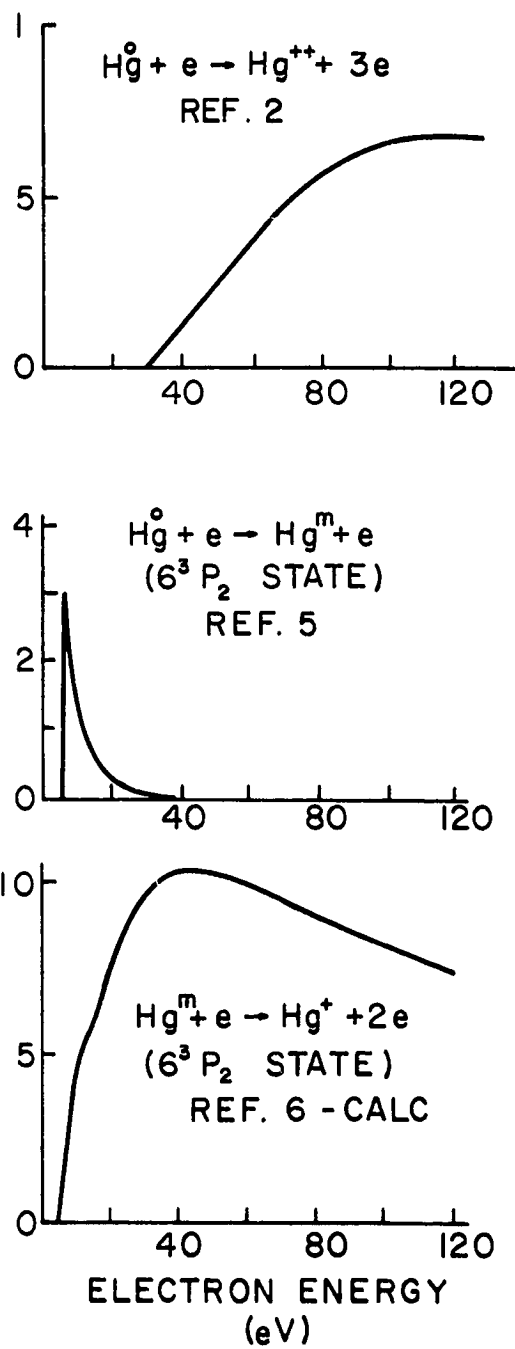
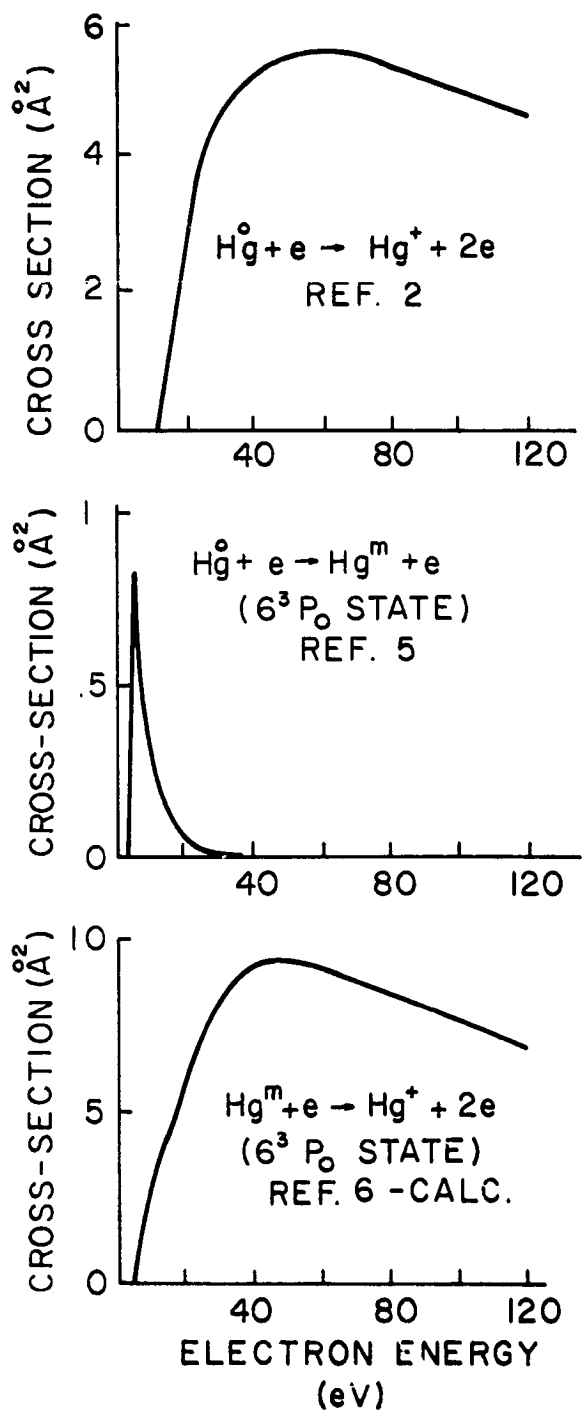


Figure 3 Mercury Cross Sections

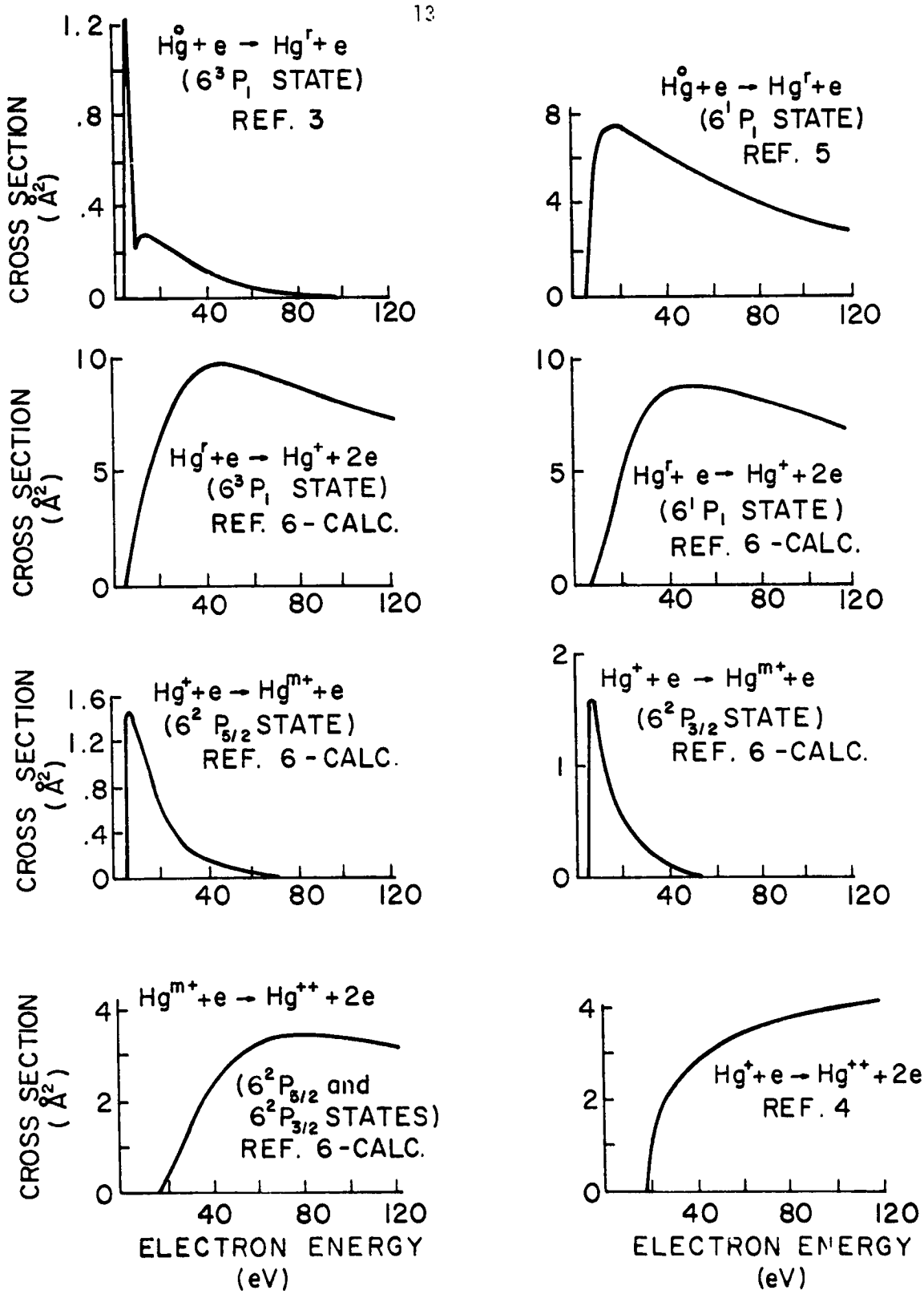


Figure 3 Mercury Cross Sections (continued)

In order to use Equation (5) to evaluate all of the production rates the volume averaged plasma properties (n_{pr}^* , n_{mx}^* , ε_{pr}^* , T_{mx}^*) must be determined. Comparing Equations (2) and (5) the following definitions of the volume averaged properties must apply.

$$n_{\alpha}^* n_{pr}^* P_{\alpha}^Y(\varepsilon_{pr}^*) \neq = \int_{Volume} n_{\alpha} n_{pr} P_{\alpha}^Y(\varepsilon_{pr}) dV \quad (6)$$

$$n_{\alpha}^* n_{mx}^* Q_{\alpha}^Y(T_{mx}^*) \neq = \int_{Volume} n_{\alpha} n_{mx} Q_{\alpha}^Y(T_{mx}) dV \quad (7)$$

These two equations show that the volume averaged plasma properties will be weighted in some manner. In order to evaluate the integrals, species α and γ must be chosen. The only specie density (n_{α}) that can be determined readily is the single ion density because plasma neutrality requires it to be approximately equal to the electron density. Specie γ must also be chosen in order to determine what P_{α}^Y and Q_{α}^Y to use. Figure 2 shows only two choices are possible--the singly ionized metastable states and the doubly ionized ground state. Since the whole purpose of the model is to determine the double ion density, specie γ was chosen as the doubly ionized ground state. Using these choices for species α and γ , Equations (6) and (7) were rewritten in the following form where the electron density (n_e) has been used to approximate the single ion density.

$$n_e^* n_{pr}^* P_+^{++}(\varepsilon_{pr}^*) \neq = \int_{Volume} n_e n_{pr} P_+^{++}(\varepsilon_{pr}) dV \quad (8)$$

$$n_e^* n_{mx}^* Q_+^{++}(T_{mx}^*) \neq = \int_{Volume} n_e n_{mx} Q_+^{++}(T_{mx}) dV \quad (9)$$

The volume averaged values of the primary electron energy (ε_{pr}^*) and the Maxwellian electron temperature (T_{mx}^*) were defined as shown in Equations (10) and (11). These definitions were chosen because they give reasonable values for the properties involved (i.e. these volume averaged values can't be greater than the peak values, which was possible with some of the other definitions).

$$P_+^{++}(\varepsilon_{pr}^*) = \frac{\int_{\text{Volume}} n_e n_{pr} P_+^{++}(\varepsilon_{pr}) dV}{\int_{\text{Volume}} n_e n_{pr} dV} \quad (10)$$

$$Q_+^{++}(T_{mx}^*) = \frac{\int_{\text{Volume}} n_e n_{mx} Q_+^{++}(T_{mx}) dV}{\int_{\text{Volume}} n_e n_{mx} dV} \quad (11)$$

Equations (8) - (11) along with Equation (12), which says the volume averaged electron density is the sum of the volume averaged primary and Maxwellian electron densities, can be combined to obtain the following definitions of the remaining volume averaged plasma properties.

$$n_e^* = n_{pr}^* + n_{mx}^* \quad (12)$$

$$n_e^* = \left[\int_{\text{Volume}} n_e^2 dV \right]^{1/2} / V^{1/2} \quad (13)$$

$$n_{pr}^* = \frac{\int_{\text{Volume}} n_e n_{pr} dV}{\left[\int_{\text{Volume}} n_e^2 dV \right]^{1/2} V^{1/2}} \quad (14)$$

$$n_{mx}^* = \frac{\int_{\text{Volume}} n_e n_{mx} dV}{\left[\int_{\text{Volume}} n_e^2 dV \right]^{1/2} V^{1/2}} \quad (15)$$

This concludes the mathematical development for electron bombardment reactions.

The volume averaged plasma properties must be evaluated in order to use Equation (5) to calculate the production rates. The plasma properties (n_{pr} , n_{mx} , ϵ_{pr} , T_{mx}) are measured at many points inside the discharge chamber by a Langmuir probe. This data is then used to evaluate the integrals in Equations (10), (11) and (13)-(15) numerically yielding the needed volume averaged plasma properties.

Migration Losses

The second type of process to be considered is that of an excited atom or ion going to the plasma boundary. The equation for the plasma boundary loss rate of a specie α is given by:

$$R_{\ell\alpha} = \int_{\text{plasma boundary}} n_\alpha v_\alpha dA \quad (16)$$

where n_α is the density of specie α at the boundary, v_α is its average velocity toward the plasma boundary, and dA is the infinitesimal area. For neutral particles assumed to have a temperature equal to the discharge chamber wall temperature and having a mass " m_0 " the average velocity toward the boundary (v_0) is equal to one-fourth the average thermal speed

$$v_0 = \frac{1}{4} \sqrt{\frac{8k T_{\text{wall}}}{\pi m_0}} \quad (17)$$

where k is the Boltzmann constant.

For ions this velocity is determined by the Bohm criterion^(8,9) and is given by

$$v_q = \sqrt{\frac{T_{mx}q}{m_i}} (1 + \frac{n_{pr}}{n_{mx}}) \quad (18)$$

where q is the ion charge (coul) and m_i is the ion mass (kg), and T_{mx} , n_{pr} and n_{mx} are as defined previously.

Since the integral equation used to define production rates has been reduced to an algebraic equation in terms of average properties Equation (16) should also be simplified in this manner. Because the migration loss is a surface phenomenon, however, it is necessary to use surface averaged densities and velocities based on surface average properties to obtain

$$R_{l\alpha} = n_\alpha^S v_\alpha^S A \quad (19)$$

where A is the total surface area of the primary electron region and the superscript "s" designates values based on surface averaged properties. Equation (19) could be made more convenient for use in the model if it were based on volume averaged properties as Equation (5) is. Equation (19) was for this reason rewritten in terms of volume averaged densities as follows

$$R_{l\alpha} = n_\alpha^* v_\alpha^* A/F_\alpha \quad (20)$$

where v_α^* is $v_q(T_{mx}^*, n_{pr}^*/n_{mx}^*)$ and F_α is a plasma uniformity factor given by Equation (21) which relates the volume and surface averaged density-velocity product.

$$F_{\alpha} = \frac{n_{\alpha}^* v_{\alpha}^*}{n_{\alpha}^S v_{\alpha}^S} = \frac{n_{\alpha}^* v_{\alpha}^*}{\left[\int n_{\alpha}^* v_{\alpha}^* dA \right] / A} \quad (21)$$

plasma boundary

This concludes the mathematical development for the migration loss of excited species, but some additional discussion and quantification of the uniformity factor F_{α} is necessary before it can be used in Equation (20). The evaluation of F_{α} for neutral excited states is difficult because it is difficult to measure their densities. The migration of excited neutrals to the plasma boundary is however a minor loss mechanism compared to the losses due to the conversion of neutral excited atoms into single ions. Therefore F_{α} for neutral excited states can be set equal to unity without introducing a significant error into the total loss rate calculation. In the case of ions, however, migration to the boundary is a major loss mechanism and F_{α} must be evaluated in order to obtain accurate results. For the singly ionized ground state the approximation, $n_+ = n_e$, can again be used in order to evaluate F_+ using Equation (21). The uniformity factor for the singly ionized metastable states was set to unity since these states have a very minor effect on the double ion density. The determination of F_{++} is based on the observation⁽¹⁰⁾ that the volume averaged double ion density (n_{++}^*) is proportional to the volume averaged electron density squared (n_e^*)². It has been assumed that this proportionality holds locally and this results in the following definition of F_{++} .

$$F_{++} = \frac{(n_e^*)^2 v_{++}^*}{\left[\int n_e^* v_{++}^* dA \right] / A} \quad (22)$$

plasma boundary

Photon Diffusion Losses

The third type of process to be considered is the loss of resonance state atoms due to photon diffusion to the walls of the discharge chamber. From diffusion theory the rate of photon loss across any plasma boundary and hence the rate of resonance state atom loss by this mechanism is given by the equation

$$R_{\text{dr}} = \int_{\text{plasma boundary}} D \Delta n_p \, dA = DA[\Delta n_p] . \quad (23)$$

In this equation n_p is the photon density and D is the photon diffusion coefficient which is given by

$$D = \frac{1}{3\tau(n_0^* \sigma_c)^2} \quad (24)$$

" τ " in this equation is the average lifetime of the resonance state atom, n_0^* is the neutral ground state atom density, and σ_c is the cross section for absorption of the photons by neutral ground state atoms. (11) The second equality in Equation (23) reflects the fact that average properties are being used in this analysis. The photon density has been assumed constant up to a point one photon mean free path from the boundary. From this point the density is assumed to decay linearly to zero at the boundary. This assumption yields the following conservative estimate for the photon loss rate

$$R_{\text{dr}} = DA n_p^* / \epsilon_f \quad (25)$$

where ϵ_f is the mean free path for photon absorption ($\frac{1}{n_0^* \sigma_c}$). This

approximation is valid when the photon mean free path is much less than the characteristic dimension of the plasma, a condition that is readily satisfied for this case where the photon mean free paths are very small ($\lambda_f < .1 \text{ cm}$).

Since the neutral density is assumed uniform over the discharge region the photon density profile is similar to the resonance state atom density profile and the following approximation between the photon and resonance state atom density at any location in the plasma applies:

$$n_p = n_r \beta . \quad (26)$$

β is a proportionality constant that can be thought of as the ratio of the probability that a photon will be "free" in the plasma to the probability that it will be "bound" forming a resonance state atom. This ratio of probabilities can also be expressed as the ratio of the average lifetime of a free photon ($\frac{1}{\kappa}$) to the resonance state atom lifetime (τ). Therefore, β is given by:

$$\beta = \frac{\frac{1}{\kappa}}{cn_0^{\text{res}} c} \quad (27)$$

where c is the speed of light and the other quantities have already been defined. Combining Equations (25), (26) and (27) one obtains the following equation for the loss rate of resonance state atoms due to photon diffusion:

$$R_{\text{loss}} = \frac{n_r^*}{3c} A \left[-\frac{1}{n_0^{\text{res}}} \right] . \quad (28)$$

Determination of Specie Densities

The equations derived so far in this section can now be combined to determine the equilibrium density of each specie included in the model. Equations of the form of (5) and (20) -- and (28) for the case of resonance state atoms -- along with the values for the volume averaged plasma properties and the plasma uniformity factors can be used to determine the rates of production and loss for each specie in the plasma. The steady state density of these species can then be calculated by equating their total production rates to their total loss rates. For example, the 6^3P_0 metastable atom density is determined by equating the production rate of this metastable atomic state from neutral ground state atoms to the sum of the associated loss rates due to 1) migration to the wall, 2) production of single ions, and 3) the production of double ions, that is

$$\begin{aligned} n_0^* [n_{pr}^* P_0^m(\xi_{pr}^*) + n_{mx}^* Q_0^m(T_{mx}^*)] \neq & \frac{n_m^* v_m^* A}{F_m} \\ + n_m^* [n_{pr}^* P_m^+(\xi_{pr}^*) + n_{mx}^* Q_m^+(T_{mx}^*)] \neq & + n_m^* [n_{pr}^* P_m^{++}(\xi_{pr}^*) + n_{mx}^* Q_m^{++}(T_{mx}^*)] \neq . \end{aligned} \quad (29)$$

Solving this for the metastable atom density ratio one obtains

$$\begin{aligned} \frac{n_m^*}{n_0^*} = & [n_{pr}^* P_0^m(\xi_{pr}^*) + n_{mx}^* Q_0^m(T_{mx}^*)] / \left\{ \frac{v_m^*}{A F_m} + [n_{pr}^* P_m^+(\xi_{pr}^*) \right. \\ & \left. + n_{mx}^* Q_m^+(T_{mx}^*)] + [n_{pr}^* P_m^{++}(\xi_{pr}^*) + n_{mx}^* Q_m^{++}(T_{mx}^*)] \right\} \end{aligned} \quad (30)$$

where n_m^* is the volume average metastable state density and v_m^* is the average velocity of metastable neutral atoms toward the boundary. A similar type of equation can be derived for each of the other excited states but they are all as complex or more complex than Equation (30).

For example, the equation for the doubly ionized ground state density has eight terms in the numerator. Each of these terms has the same form as the bracketted quantities in the numerator of Equation (30).

The quantity $\#/\Lambda$ in the denominator of Equation (30) has an interesting physical interpretation. It is contained in a term which represents the loss rate per unit volume of metastable state atoms to the plasma boundary. This term shows the manner in which the size and shape of the primary electron region enters into the model. For a large thruster $\#/\Lambda$ will be large and an ion or excited neutral must, on the average, travel great distances to reach the plasma boundary, and so the loss rate per unit volume of these species will be small. For a small thruster $\#/\Lambda$ will be small and on the average the ions and excited species are near the boundary and can reach it readily resulting in a large loss rate of these species per unit volume.

At this point only the relative density of each excited species (n_α^*/n_0^*) can be calculated. However one additional fact can be added to the model, the requirement that the plasma be neutral (i.e., $n_e^* = n_+^* + n_{m+}^* + 2n_{++}^*$). This requirement when added to the relative density equations of the ionized states implies unique single, metastable single and double ion densities. These in turn imply a unique neutral atom density and hence a unique density for each species considered in the analysis. One must however iterate to arrive at these densities because a neutral ground state atom density must be assumed initially to determine photon loss rates from Equation (28). At the conclusion of the analysis then the calculated ground state atom density must agree with the assumed value.

A computer program has been written which calculates the densities of all the species considered in the model. The densities are calculated by using relative density equations similar to Equation (30) and the plasma neutrality condition. The input needed to make these calculations includes the volume averaged plasma properties, the plasma uniformity factors and the volume-to-surface area ratio of the primary electron region. A listing of this computer program entitled "HG" is included as Appendix A.

EXPERIMENTAL PROCEDURES AND RESULTS

The model developed in the previous section will predict the specie densities if the volume averaged plasma properties, uniformity factors and geometric quantities, which are collectively called the input parameters, are known. In order to verify the accuracy of the model, data must be gathered so that the model's input parameters can be determined. These input parameters can be used by the model to predict the specie densities which can then be compared to the measured densities to determine the model's accuracy. The model's accuracy has been determined by comparing the measured and predicted double ion densities since the double ion density is the model's main concern.

In order to test the accuracy of the model over a wide range of conditions data were used from different thrusters and operating conditions. The 15 cm diameter SERT II thruster was operated with two different grid sets and at three different power levels in each of these configurations. Data were collected at each condition allowing the accuracy of the model to be verified at six different points. Data for the 30 cm diameter thruster were also obtained from Hughes Research Laboratories⁽¹²⁾ so that the model could be verified over a wider range of thruster sizes, configurations, and operating conditions. Both thrusters have strongly divergent magnetic fields. Their general configuration and manner of operation have been described in the "Thruster Operation" section. More detailed thruster specifications, etc. are available in the literature.^(9, 13, 14)

The data gathering procedure for the 15 cm thruster will be used to illustrate the general manner in which the needed data were obtained.

Before the gathering of data could begin thruster operation and flow rates were kept stable for approximately thirty minutes. This insured thruster conditions would change little in the twenty minute period during which the data were obtained. Table I lists the conditions and configurations at which the 15 cm thruster was operated at C.S.U. along with those for the 30 cm thruster as obtained from Hughes Research Laboratories. This table indicates the changes in configuration for both thrusters resulted from using different grid types. The SERT II grids, listed in Table I, are flat grids with hole diameters of $\approx .4$ cm and in operation are separated by a gap of .23 cm. The high permeance dished grids are dished slightly to prevent the grids from shorting during operation due to their thermal expansion. Their hole diameter is smaller (.25 cm) as is their separation gap (.079). More detailed specifications for the two grid types can be found in Reference 9. The EM (Engineering Model) grids are similar to the high permeance dished grids described above. The SHAG (Small Hole Accelerator Grids) grids have an accelerator hole diameter that is $\approx 70\%$ of the EM grids' accelerator hole diameter. This smaller hole size reduces the loss of neutral propellant. These two grid types are described in more detail in References 15 and 16. Table I shows, for example, that the 15 cm thruster with the SERT II grids was operated at one condition where the amount of current collected at the anode (I_{arc}) was 1.7A, while the voltage difference between the anode and cathode (V_{arc}) was 37.2 V and the ion current through the grids (I_{beam}) was 0.258 A.

The values of the volume averaged plasma properties and the uniformity factors must be known in order to calculate the theoretical double ion density. In order to determine the values of these average

Table I
Thruster Sizes, Configurations and Conditions

Thruster Diameter (cm)	Grid Type	Anode Current (I_{arc} --A)	Anode Voltage (V_{arc} --V)	Ion Beam Current (I_{beam} --A)	Mass Flow Rate (A)
15.	SERT II	1.00	33.	.180	.310
15.	SERT II	1.70	37.2	.258	.307
15.	SERT II	2.05	42.6	.272	.308
15.	Dished	3.02	32.2	.499	.735
15.	Dished	4.06	37.5	.654	.725
15.	Dished	4.13	40.4	.622	.650
30.	EM	5.0	37.	1.0	1.25
30.	EM	7.5	37.	1.5	1.76
30.	EM	10.0	37.	2.0	2.29
30.	SHAG	9.5	30.	1.5	1.74
30.	SHAG	11.7	30.	2.0	2.30

plasma properties, the primary and Maxwellian electron densities and energies must be determined everywhere in the discharge chamber. The plasma properties at some point in the plasma can be measured using a Langmuir probe and analyzed using the procedure described in Reference 17. The plasma properties at sixteen different points in the plasma were measured, for each 15 cm thruster condition listed in Table I, using the movable Langmuir probe and associated circuitry described in Reference 18. The results of a typical survey (15 cm thruster - SERT II grids -37 V anode voltage) are plotted in Figure 4. This figure shows the spatial variation of the Maxwellian electron temperature, primary electron energy and the primary and Maxwellian electron densities in the discharge chamber. The Maxwellian electron temperature is seen to average approximately 9 eV over the primary electron region defined by the critical field line while the primary electron energy averages about 30 eV. The average Maxwellian electron density is about 10^{11} cm^{-3} while the average primary electron density is approximately 10^{10} cm^{-3} over the same region. The electron densities and energies are seen to be fairly uniform in the primary electron region but drop off rapidly outside this region. Using data similar to that plotted in Figure 4, Equations (10)-(15) and (21) were evaluated numerically by the computer program "PROP" (listed in Appendix B) to obtain the volume averaged properties and uniformity factors for each case. The results are listed in Table II along with the volume-to-surface area ratio of the primary electron region (Ψ/A) and the thruster operating specifications which are reproduced from Table I. The average values which resulted from an examination of Figure 4 ($T_{mx} = 9 \text{ eV}$, $E_{pr} = 30 \text{ eV}$, $n_{mx} = 10^{11} \text{ cm}^{-3}$, $n_{pr} = 10^{10} \text{ cm}^{-3}$) are seen to

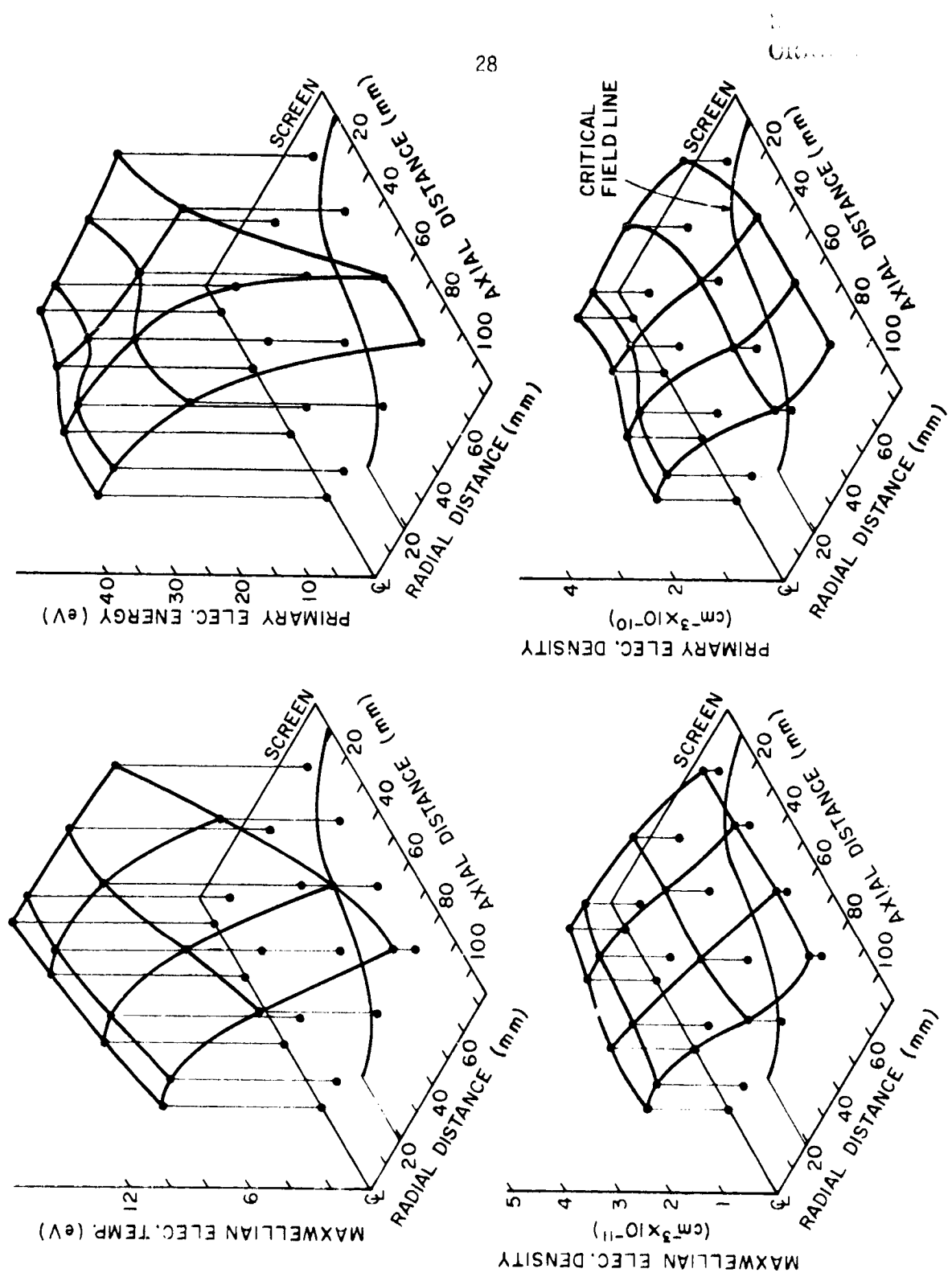


Figure 4 Plasma Property Profiles, 15 cm Thruster -
CRT II Grids - 37 V Anode Voltage

Table II
Experimental Results

	15.	15.	15.	15.	15.	15.	30.	30.	30.	30.	30.	30.
Thruster Diameter (cm)		SERT II		HIGH PERMEANCE DISHED		EM	EM	EM	EM	SHAG	SHAG	
Grid Type	1.0	1.7	2.05	3.02	4.06	4.13	5.0	7.5	10.0	9.5	11.7	
Anode Current (I_{arc} --A)	33.	37.2	42.6	32.2	37.5	40.4	37.	37.	37.	30.	30.	
Anode Voltage (V_{arc} --V)	.190	.258	.272	.499	.654	.622	1.0	1.5	2.0	1.5	2.0	
Beam Current (I_{beam} --A)	.310	.307	.308	.735	.725	.650	1.25	1.76	2.29	1.74	2.30	
Mass Flow Rate (A)												
Plasma Volume to Surface	1.4	1.4	1.4	1.4	1.4	1.4	2.5	2.5	2.5	2.5	2.5	2.5
Area Ratio ($\pi/4$ --cm ²)												
Average Maxwellian Electron Temperature (T_{ex} --eV)	4.2	9.1	12.2	4.3	7.1	10.2	3.3	3.6	3.8	3.0	2.9	
Average Primary-to-Maxwellian Electron Density Ratio (n_{pr}^*/n_{mx}^*)	.034	.033	.166	.017	.042	.134	.50	.35	.25	.19	.22	
Average Primary Electron Energy (E_{pr} --eV)	27.5	29.6	38.4	21.5	23.4	31.0	25.4	25.5	27.2	19.6	19.7	
Average Electron Density ($n_e \times 10^{15}$ cm ⁻³)	9.80	9.10	8.07	36.0	24.3	18.2	7.51	8.97	16.4	8.3	12.8	
Input Power (W)												
Uniformity Factor F_+	2.3	2.1	2.3	2.0	1.9	1.8	1.5	1.5	1.5	1.8	1.7	
Uniformity Factor F_{++}	3.1	2.5	2.6	2.5	2.1	2.0	1.8	1.9	1.8	2.5	2.1	
Measured Double-to-Single Ion Current Ratio (I_{++}/I_+)	.024	.073	.12	.036	.081	.18	.080	.125	.167	.062	.080	

agree well with the volume averaged values listed in Table II ($T_{\text{mx}}^* = 9.1 \text{ eV}$, $\epsilon_{\text{pr}}^* = 29.6 \text{ eV}$, $n_{\text{mx}}^* = 8.4 \times 10^{19} \text{ cm}^{-3}$, $n_{\text{pr}}^* = 7.0 \times 10^{19} \text{ cm}^{-3}$). F_+ and F_{++} , which are defined as the ratio of the volume average ion flux to the average flux at the surface of the primary electron region, are seen to have values of 2.1 and 2.5 respectively for the case being discussed. The average plasma properties listed in Table II are observed to cover a wide range in plasma conditions; a situation which is desirable for verification of the model.

The double ion density inside the discharge chamber must also be determined. This can be accomplished indirectly by determining the double-to-single ion density ratio (n_{++}/n_+) in the discharge chamber and the single ion density. The single ion density can be determined with sufficient accuracy by equating the single ion density to the electron density. The value of the double-to-single ion density ratio can be determined from measurements of the ratio of the double ion current to the single ion current in the exhaust beam (I^{++}/I^+), and the equation

$$n_{++}/n_+ = \frac{I^{++}}{I^+ \cdot 2\sqrt{2}} . \quad (31)$$

The quantity $2\sqrt{2}$ accounts for charge and Bohm criterion velocity differences between double and single ions.

The quantity " I^{++}/I^+ " was measured using a mass spectrometer⁽¹⁹⁾. The methods used for data acquisition and analysis using such a device are described in Reference 20 for the 15 cm thruster data and in Reference 19 for the 30 cm thruster. The results obtained are listed in the last row of Table II. They show, for example, a double-to-single ion current ratio of 2.3 for the 30 cm thruster - NEPC II grid - 37 V

anode voltage case. The general trend observed from these data is that an increase in power input (I_{arc} times V_{arc}) for a certain thruster configuration results in an increase in the ratio I^{++}/I^+ .

RESULTS AND DISCUSSION

The values of the average plasma properties, listed in Table II, are observed to vary over large ranges. For example, the average Maxwellian electron temperature ranges from a low value of 3.3 eV to a high value of 12.2. Similarly the average primary-to-Maxwellian electron density ratio varies from 0.02 to 0.50. This large variation is considered sufficient to allow a general decision to be made about the accuracy of the model. Comparisons of the experimental and theoretical values of the double-to-single ion density ratio have been used to verify the model's accuracy because this quantity (n_{++}/n_+) was determined experimentally. The theoretical and experimental values of the double-to-single ion density ratio are plotted as a function of propellant utilization in Figures 5 and 6. The curves labeled "THEORETICAL" result from predictions made by the model using the "Input Parameters" listed in Table II. The curves labeled "EXPERIMENTAL" result from measurements of the ratio I^{++}/I^+ made using the mass spectrometer. The trends exhibited by the THEORETICAL and EXPERIMENTAL curves are very similar and the agreement between the THEORETICAL and EXPERIMENTAL values of the double-to-single ion density ratio is good for plasma physics work with the average error being 3%. The maximum error of 40% is observed at low double-to-single ion density ratios in the 30 cm thruster. These error values indicate the model is accurate over a wide range of plasma conditions and thruster configurations.

Since the model has been shown to be accurate in its predictions of the double-to-single ion density ratio over a wide range of conditions there is a distinct possibility that the specie densities and

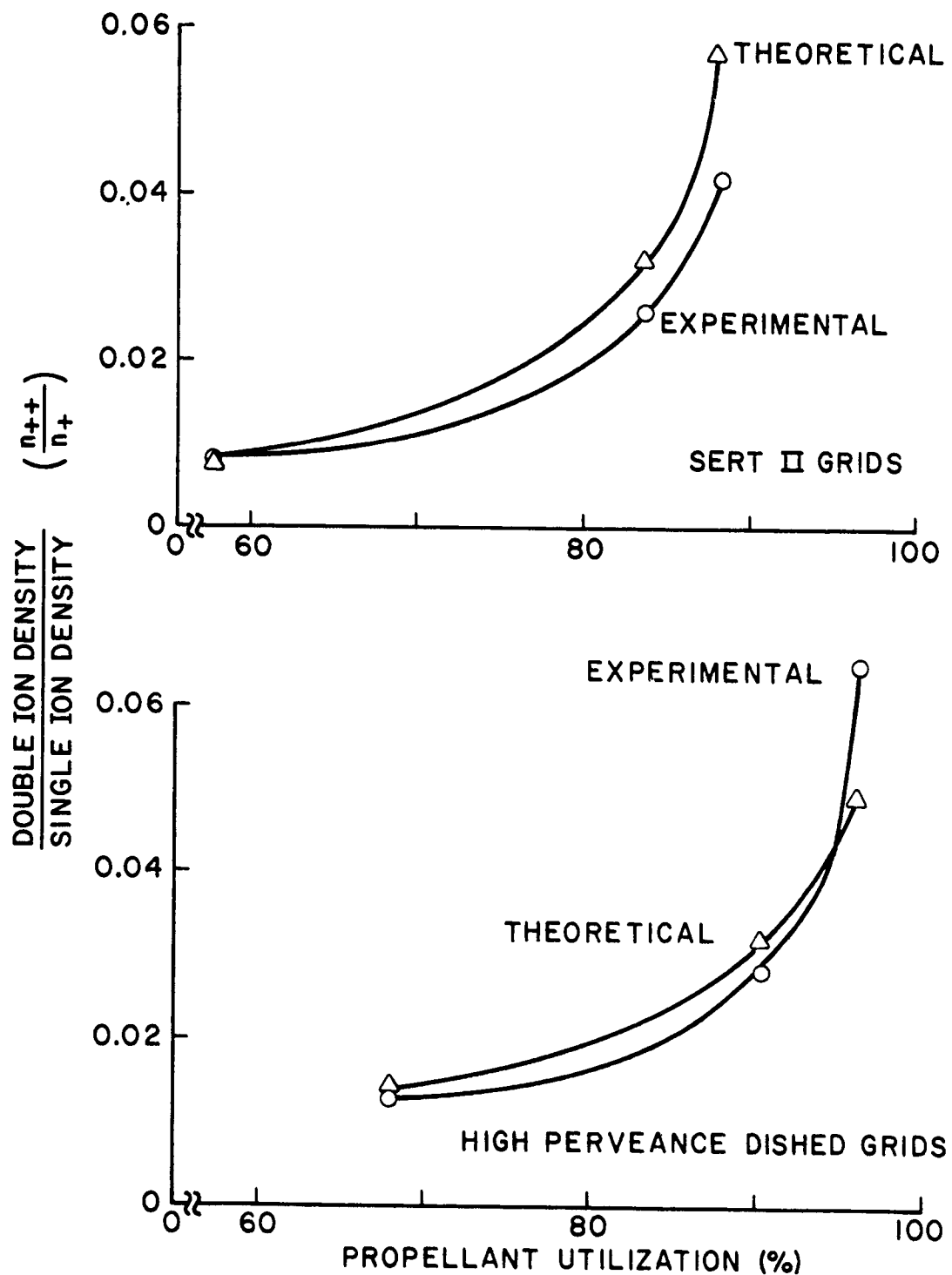


Figure 5 Double-to-Single Ion Density Ratio in a
15 cm Diameter Thruster

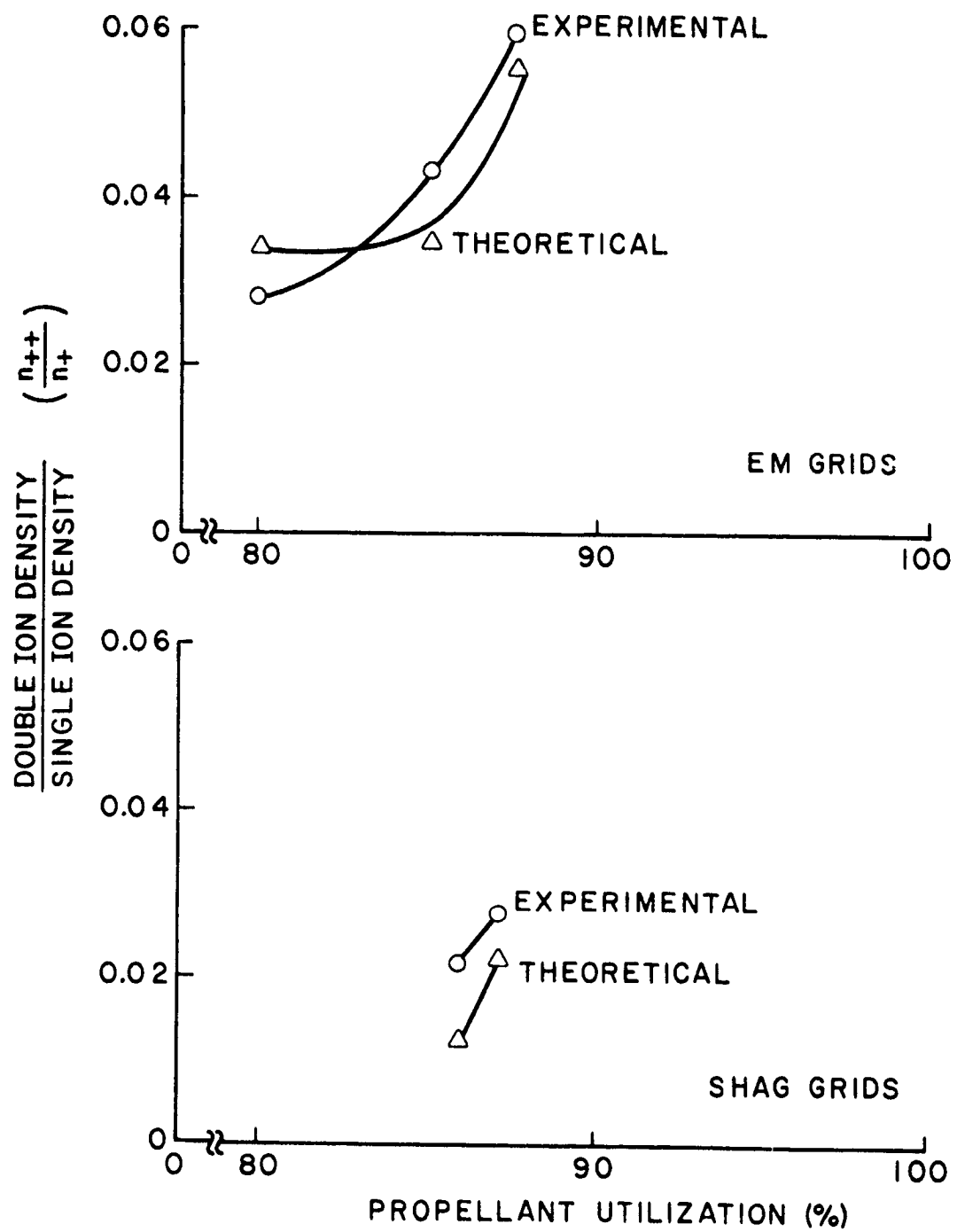


Figure 6 Double-to-Single Ion Density Ratio in a
30 cm Diameter Thruster

reaction rates used to predict the double-to-single ion density ratio are also accurate. The remainder of this section will examine the model's predictions of these specie densities and reaction rates. These quantities are listed in Table III along with the thruster operating variables and the model's input parameters which were reproduced from Table II.

The section in Table III titled "Calculated Normalized Densities" lists the model's predictions of the normalized densities of the states considered in the model where the normalized density of some specie is defined as the specie density divided by the total heavy particle density. The sum of the normalized densities for any thruster condition should therefore equal unity. Table III shows, for example, that the 15 cm diameter thruster operating with SERT II grids at 37 V anode voltage would be predicted to have 68% neutral ground state atoms, 19% neutral resonance state atoms, 6.9% singly charged ground state ions and .2% doubly charged ground state ions. The normalized density of the single ions agrees fairly well in all cases with the 10% value quoted as typical in the literature.⁽¹⁾ As expected the neutral ground state atoms are the most numerous.

These normalized density trends can be explained in terms of variations of plasma properties. For example, the normalized single ion density increases with increasing power input (I_{arc} times V_{arc}) to the thruster in all cases. This occurs because an increase in the values of the volume averaged plasma properties causes the ratio of the production rate of single ions to the total neutral density to increase. The increase in the ratio indicates a smaller total neutral density is

Table III
Predicted Densities and Reaction Rates

Operative Variables	15	25	35	45	55	65	75	85	95	105	115	125	135	145	155	165	175	185	195	205	215	225	235	245	255	265	275	285	295	305	315	325	335	345	355	365	375	385	395	405	415	425	435	445	455	465	475	485	495	505	515	525	535	545	555	565	575	585	595	605	615	625	635	645	655	665	675	685	695	705	715	725	735	745	755	765	775	785	795	805	815	825	835	845	855	865	875	885	895	905	915	925	935	945	955	965	975	985	995	1005	1015	1025	1035	1045	1055	1065	1075	1085	1095	1105	1115	1125	1135	1145	1155	1165	1175	1185	1195	1205	1215	1225	1235	1245	1255	1265	1275	1285	1295	1305	1315	1325	1335	1345	1355	1365	1375	1385	1395	1405	1415	1425	1435	1445	1455	1465	1475	1485	1495	1505	1515	1525	1535	1545	1555	1565	1575	1585	1595	1605	1615	1625	1635	1645	1655	1665	1675	1685	1695	1705	1715	1725	1735	1745	1755	1765	1775	1785	1795	1805	1815	1825	1835	1845	1855	1865	1875	1885	1895	1905	1915	1925	1935	1945	1955	1965	1975	1985	1995	2005	2015	2025	2035	2045	2055	2065	2075	2085	2095	2105	2115	2125	2135	2145	2155	2165	2175	2185	2195	2205	2215	2225	2235	2245	2255	2265	2275	2285	2295	2305	2315	2325	2335	2345	2355	2365	2375	2385	2395	2405	2415	2425	2435	2445	2455	2465	2475	2485	2495	2505	2515	2525	2535	2545	2555	2565	2575	2585	2595	2605	2615	2625	2635	2645	2655	2665	2675	2685	2695	2705	2715	2725	2735	2745	2755	2765	2775	2785	2795	2805	2815	2825	2835	2845	2855	2865	2875	2885	2895	2905	2915	2925	2935	2945	2955	2965	2975	2985	2995	3005	3015	3025	3035	3045	3055	3065	3075	3085	3095	3105	3115	3125	3135	3145	3155	3165	3175	3185	3195	3205	3215	3225	3235	3245	3255	3265	3275	3285	3295	3305	3315	3325	3335	3345	3355	3365	3375	3385	3395	3405	3415	3425	3435	3445	3455	3465	3475	3485	3495	3505	3515	3525	3535	3545	3555	3565	3575	3585	3595	3605	3615	3625	3635	3645	3655	3665	3675	3685	3695	3705	3715	3725	3735	3745	3755	3765	3775	3785	3795	3805	3815	3825	3835	3845	3855	3865	3875	3885	3895	3905	3915	3925	3935	3945	3955	3965	3975	3985	3995	4005	4015	4025	4035	4045	4055	4065	4075	4085	4095	4105	4115	4125	4135	4145	4155	4165	4175	4185	4195	4205	4215	4225	4235	4245	4255	4265	4275	4285	4295	4305	4315	4325	4335	4345	4355	4365	4375	4385	4395	4405	4415	4425	4435	4445	4455	4465	4475	4485	4495	4505	4515	4525	4535	4545	4555	4565	4575	4585	4595	4605	4615	4625	4635	4645	4655	4665	4675	4685	4695	4705	4715	4725	4735	4745	4755	4765	4775	4785	4795	4805	4815	4825	4835	4845	4855	4865	4875	4885	4895	4905	4915	4925	4935	4945	4955	4965	4975	4985	4995	5005	5015	5025	5035	5045	5055	5065	5075	5085	5095	5105	5115	5125	5135	5145	5155	5165	5175	5185	5195	5205	5215	5225	5235	5245	5255	5265	5275	5285	5295	5305	5315	5325	5335	5345	5355	5365	5375	5385	5395	5405	5415	5425	5435	5445	5455	5465	5475	5485	5495	5505	5515	5525	5535	5545	5555	5565	5575	5585	5595	5605	5615	5625	5635	5645	5655	5665	5675	5685	5695	5705	5715	5725	5735	5745	5755	5765	5775	5785	5795	5805	5815	5825	5835	5845	5855	5865	5875	5885	5895	5905	5915	5925	5935	5945	5955	5965	5975	5985	5995	6005	6015	6025	6035	6045	6055	6065	6075	6085	6095	6105	6115	6125	6135	6145	6155	6165	6175	6185	6195	6205	6215	6225	6235	6245	6255	6265	6275	6285	6295	6305	6315	6325	6335	6345	6355	6365	6375	6385	6395	6405	6415	6425	6435	6445	6455	6465	6475	6485	6495	6505	6515	6525	6535	6545	6555	6565	6575	6585	6595	6605	6615	6625	6635	6645	6655	6665	6675	6685	6695	6705	6715	6725	6735	6745	6755	6765	6775	6785	6795	6805	6815	6825	6835	6845	6855	6865	6875	6885	6895	6905	6915	6925	6935	6945	6955	6965	6975	6985	6995	7005	7015	7025	7035	7045	7055	7065	7075	7085	7095	7105	7115	7125	7135	7145	7155	7165	7175	7185	7195	7205	7215	7225	7235	7245	7255	7265	7275	7285	7295	7305	7315	7325	7335	7345	7355	7365	7375	7385	7395	7405	7415	7425	7435	7445	7455	7465	7475	7485	7495	7505	7515	7525	7535	7545	7555	7565	7575	7585	7595	7605	7615	7625	7635	7645	7655	7665	7675	7685	7695	7705	7715	7725	7735	7745	7755	7765	7775	7785	7795	7805	7815	7825	7835	7845	7855	7865	7875	7885	7895	7905	7915	7925	7935	7945	7955	7965	7975	7985	7995	8005	8015	8025	8035	8045	8055	8065	8075	8085	8095	8105	8115	8125	8135	8145	8155	8165	8175	8185	8195	8205	8215	8225	8235	8245	8255	8265	8275	8285	8295	8305	8315	8325	8335	8345	8355	8365	8375	8385	8395	8405	8415	8425	8435	8445	8455	8465	8475	8485	8495	8505	8515	8525	8535	8545	8555	8565	8575	8585	8595	8605	8615	8625	8635	8645	8655	8665	8675	8685	8695	8705	8715	8725	8735	8745	8755	8765	8775	8785	8795	8805	8815	8825	8835	8845	8855	8865	8875	8885	8895	8905	8915	8925	8935	8945	8955	896

needed to maintain a specified single ion density and so the normalized single ion density increases as previously observed.

The last section in Table III shows the calculated production rates for singly and doubly charged ions through the various intermediate states. These production rates have been normalized by the total production rate of the specie indicated. The fraction of the associated interactions effected by the primary electrons is indicated in parenthesis. For example, at the 15 cm thruster's 37 V, SERT II grid operating point, 59% of the single ions are produced as a result of electron interaction with neutral ground state atoms and 28% resulted from electron bombardment of neutral resonance state atoms. The neutral ground state-to-single ionic state interactions were induced by primary electrons 23% of the time and by Maxwellian electrons the remainder (77%) of the time.

Thruster performance is determined primarily by the mechanism for the production and loss of single ions. The production of these ions is, according to this model, quite dependent on the neutral metastable and neutral resonance states which are ignored in most other analyses. The manner in which single ions are produced however differs a great deal between the two thrusters. In the 15 cm thruster most of the single ions are produced as a result of Maxwellian electron bombardment while primary electrons are unimportant because of their low densities. This indicates that for 15 cm thruster operation the primary electron region is the important reaction region because it is the region where high densities of high energy Maxwellian electrons occur. In the 30 cm thruster, however, relatively high primary electron densities exist and since the Maxwellian electron temperature is low most of the single ion

production results from primary electron bombardment. So for the 30 cm thruster the primary electron region is the important reaction region because it contains high densities of high energy primary electrons.

Table III indicates in all cases a large percentage of the double ions are produced from single ions. This is as one would expect because the minimum energy required to produce a double ion from a single ion is 18.7 eV while 29 eV is required to produce a double ion from a neutral ground state atom. As the power input to the thruster increases the number of electrons with energies greater than 29 eV increases causing the relative importance of the neutral-to-double transition to increase. The least energy is required for the production of double ions via singly ionized metastable states, but the densities of these states are so low that this production mechanism is unimportant.

SIMPLIFIED MODEL

In the previous section it has been shown that most double ions are produced as a result of electron bombardment of single ions. In order to simplify the analysis of the "Theoretical Model" section the other intermediate states for double ion production can therefore be ignored with no significant loss in the accuracy of the double ion density calculations. In the simplified model presented here the approximation is made that the total rate of production of double ions equals the rate of production of double ions from single ions. This production rate is given by:

$$R_p^{++} \approx R_{p+}^{++} = n_+^* [n_{pr}^* P_+^{++}(\xi_{pr}^*) + n_{mx}^* Q_+^{++}(T_{mx}^*)] \neq . \quad (32)$$

The total loss rate of double ions is given by the equation

$$R_{\ell_{++}} = \frac{n_{++}^* v_{++}^* A}{F_{++}} . \quad (33)$$

Equating the loss and production rates and then solving the resultant equation for the double ion density one obtains

$$n_{++}^* = n_+^* \frac{[n_{pr}^* P_+^{++}(\xi_{pr}^*) + n_{mx}^* Q_+^{++}(T_{mx}^*)]}{\frac{v_{++}^* A}{F_{++}}} \neq . \quad (34)$$

The approximation $n_e^* = n_+^*$ can now be used and Equation (18) can be substituted for the double ion velocity to obtain the following equation.

$$n_{++}^* = n_e^{*2} \frac{A}{\Lambda} F_{++} \frac{\left[\frac{n_{pr}^*}{n_e^*} P_+^{++}(\xi_{pr}^*) + \frac{n_{mx}^*}{n_e^*} Q_+^{++}(T_{mx}^*) \right]}{[T_{mx}^* q (1 + n_{pr}^*/n_{mx}^*)/m_i]^{1/2}} \quad (35)$$

The double ion density can now be determined for a given thruster operating condition using this equation and the plots of $P_+^{++}(\xi_{pr})$ and $Q_+^{++}(T_{mx})$ found in Figure 7 if the volume averaged plasma properties and the uniformity factor F_{++} are known. This equation will consistently predict lower double ion densities than the complete model since it ignores the production of double ions from neutral states and the singly ionized metastable states, but this error should generally be small. The error will be greatest for plasmas with high energy electrons which can produce double ions directly from neutral states.

The last section of Table III can be used to determine the magnitude of this error for the 11 cases considered in this study. Since the simplified model considers only the single-to-double transition the error associated with this approximation can be determined from the listed value of the percentage of double ions produced from single ions. For example, for the 15 cm-SERT II grid - 37 V anode voltage case the percentage of double ions produced from single ions is 78%. This means that the value of the double ion density predicted by the simplified model would be 78% of that predicted by the complete model. Examination of Table III indicates the double ion densities calculated using the simplified model will agree well with the complete model's predictions for all the 30 cm thruster conditions because in these cases the percentage of double ions produced from single ions is greater than 97%.

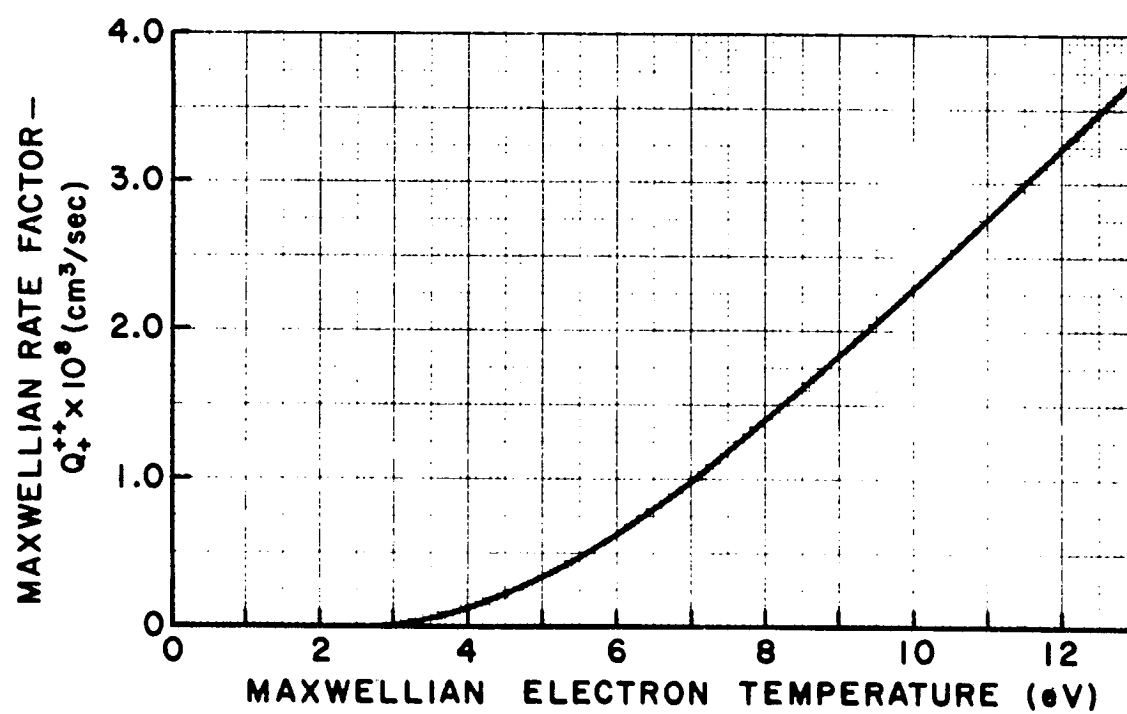
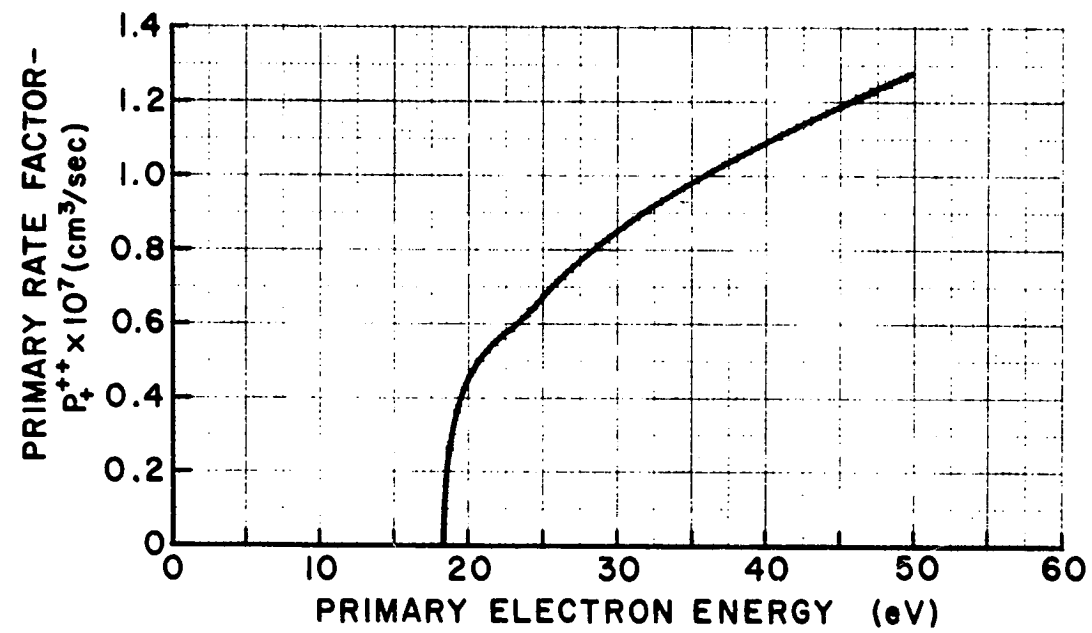
R
C

Figure 7 Rate Factors for $Hg^+ \rightarrow Hg^{++}$

In each of these cases few electrons have energies in excess of 29 eV (the minimum energy required for the neutral-to-double transition). The simplified model will however, according to Table III, yield results which are generally low for the 15 cm thruster data (e.g. 30% low for the SERT II grid - 42 V anode voltage condition) because in these cases sufficiently high Maxwellian electron temperatures exist to cause a relatively large percentage of the electrons to have energies in excess of 29 eV.

The most accurate way to determine the values of the average plasma properties required in Equation (35) would be to conduct a Langmuir probe survey of the discharge chamber under consideration to determine the plasma properties at many different points and to then use this information in Equations (10) to (15) and (21) to determine average plasma properties. The collection of the plasma property data is however costly and time consuming. For this reason average plasma property correlations were developed. The correlating parameters used are composed of thruster operating parameters (e.g. I_{arc}) and geometric properties (e.g. $\#/\text{A}$). Using the Maxwellian electron temperature data listed in Table III, for example, one obtains the correlation presented in Figure 8. The terms used in the correlating parameter are defined in Table III. The correlating parameter used in Figure 8 was determined by trial and error. The shape of a curve through the resultant data points was picked to match the trends observed in the data points. For example, the slope of the curve in the neighborhood of the low Maxwellian electron temperature points is seen to decrease. This agrees with the trend observed in the data and also agrees with a prediction, based on inelastic collision cross section data, which says a lower

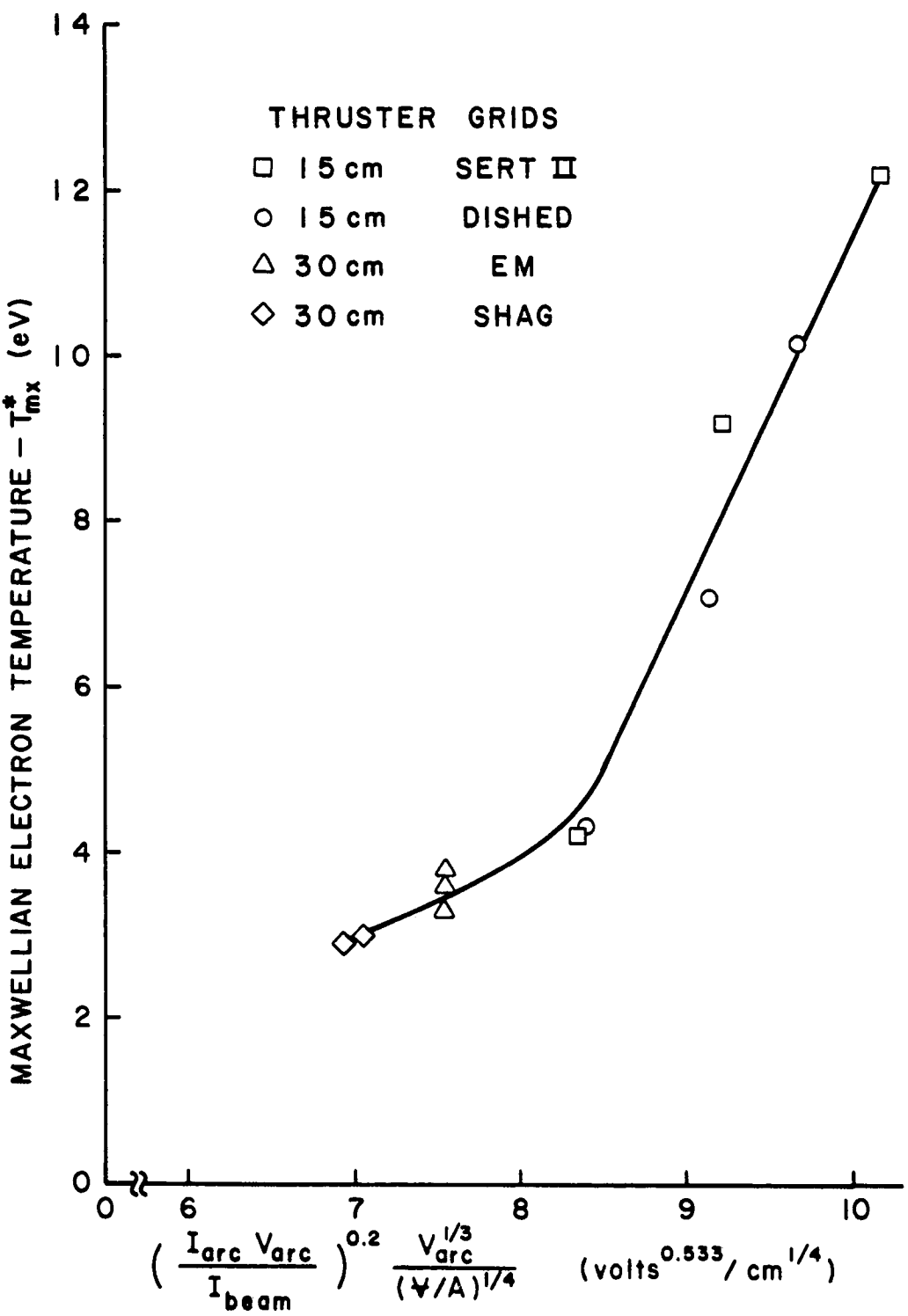


Figure 8 Maxwellian Electron Temperature Correlation

bound on the Maxwellian electron temperature should exist roughly in the neighborhood of 5 eV⁽¹⁾.

The correlation for the primary electron energy is shown in Figure 9. The correlating parameter contains the quantity n_c which is the corrected propellant utilization. The corrected utilization was used in the correlating parameter, instead of the measured propellant utilization, because a better fit of the data points resulted from its use. The propellant utilization (n) of an ion thruster depends upon the plasma properties, the effective open area for the loss of neutral atoms through the grids (A_0) and the effective open area for the loss of ions through the grids (A_+). The propellant utilization is defined by the equation

$$n = \frac{n_+ v_+ A_+}{n_+ v_+ A_+ + n_{ot} v_o A_o} \approx 1 - \frac{n_{ot} v_o A_o}{n_+ v_+ A_+} \quad (36)$$

where n_{ot} is the total neutral atom density. The primary energy (and other average plasma properties) of a given thruster correlate with the propellant utilization as defined above, but correlation between grid sets having different values of the ratio A_o/A_+ is poor. The problem caused by the utilization's dependence upon grid sets can be corrected by eliminating the ratio A_o/A_+ from Equation (36) and then substituting in its place the value of the ratio A_o/A_+ for some standard grid set. The resultant quantity is the corrected utilization and is defined by the equation

$$n_c = 1 - \frac{n_{ot} v_o}{n_+ v_+} \left[\frac{A_o}{A_+} \right]_{\text{standard}} \quad (37)$$

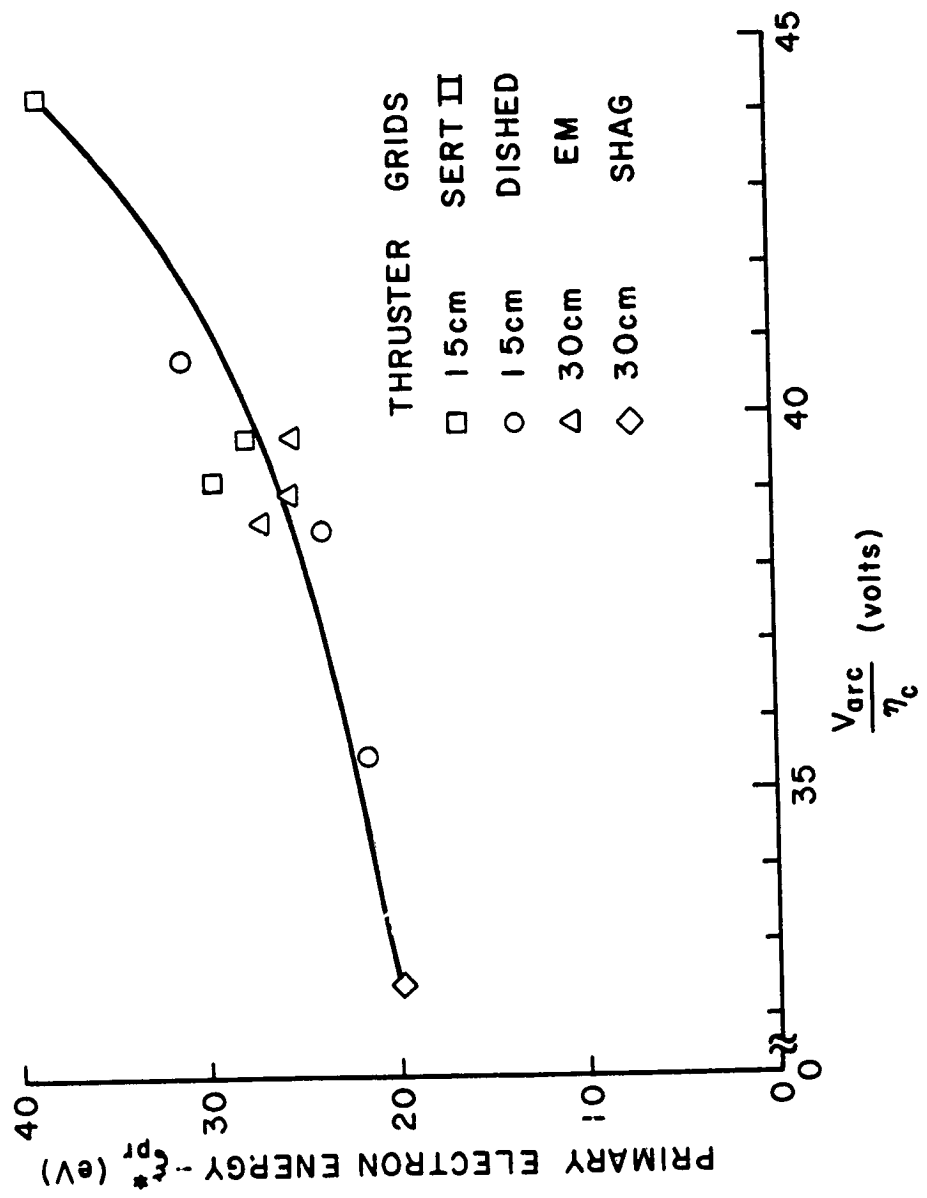


Figure 9 Primary Electron Energy Correlation

The open area for the loss of ions (A_+) from a thruster is proportional to the open area fraction of the screen grid (ϕ_s)⁽¹⁾. Equilibrium flow theory⁽¹⁾ can be used to determine that the open area for the loss of neutral atoms (A_0) is proportional to the quantity $(\phi_s \phi_a)/(\phi_s + \phi_a)$ where ϕ_a is the open area fraction of the accelerator grid. These two approximations can be used to define the ratio A_0/A_+ as follows

$$\frac{A_0}{A_+} = \left(\frac{\phi_s \phi_a}{\phi_s + \phi_a} \right) / \phi_s = \frac{\phi_a}{\phi_s + \phi_a} . \quad (38)$$

If Equations (36) - (38) are combined the following result is obtained,

$$\eta_c = 1 - .5(1 - \eta) \frac{\phi_s + \phi_a}{\phi_a} , \quad (39)$$

where the constant ".5" defines $\phi_a/(\phi_s + \phi_a)$ for the standard grid set.

Figures 10-12 show correlations for the remaining input parameters. These correlations were developed by trial and error in a manner similar to that used to obtain those in Figures 8 and 9. It should be noted that the correlation in Figure 11 is for the quantity $n_{pr}^* [\psi/A]^{-1.5}$ not the primary electron density (n_{pr}^*).

It should be understood that the correlations of Figures 8-12 are based on data obtained from strongly divergent magnetic field thrusters. The average plasma properties predicted using these figures may be inaccurate for other types of thrusters (e.g. multipole or radial field thrusters). Therefore Langmuir probe surveys should be made for these other types in order to obtain good estimates of the average plasma properties and hence accurate predictions of the double ion density.

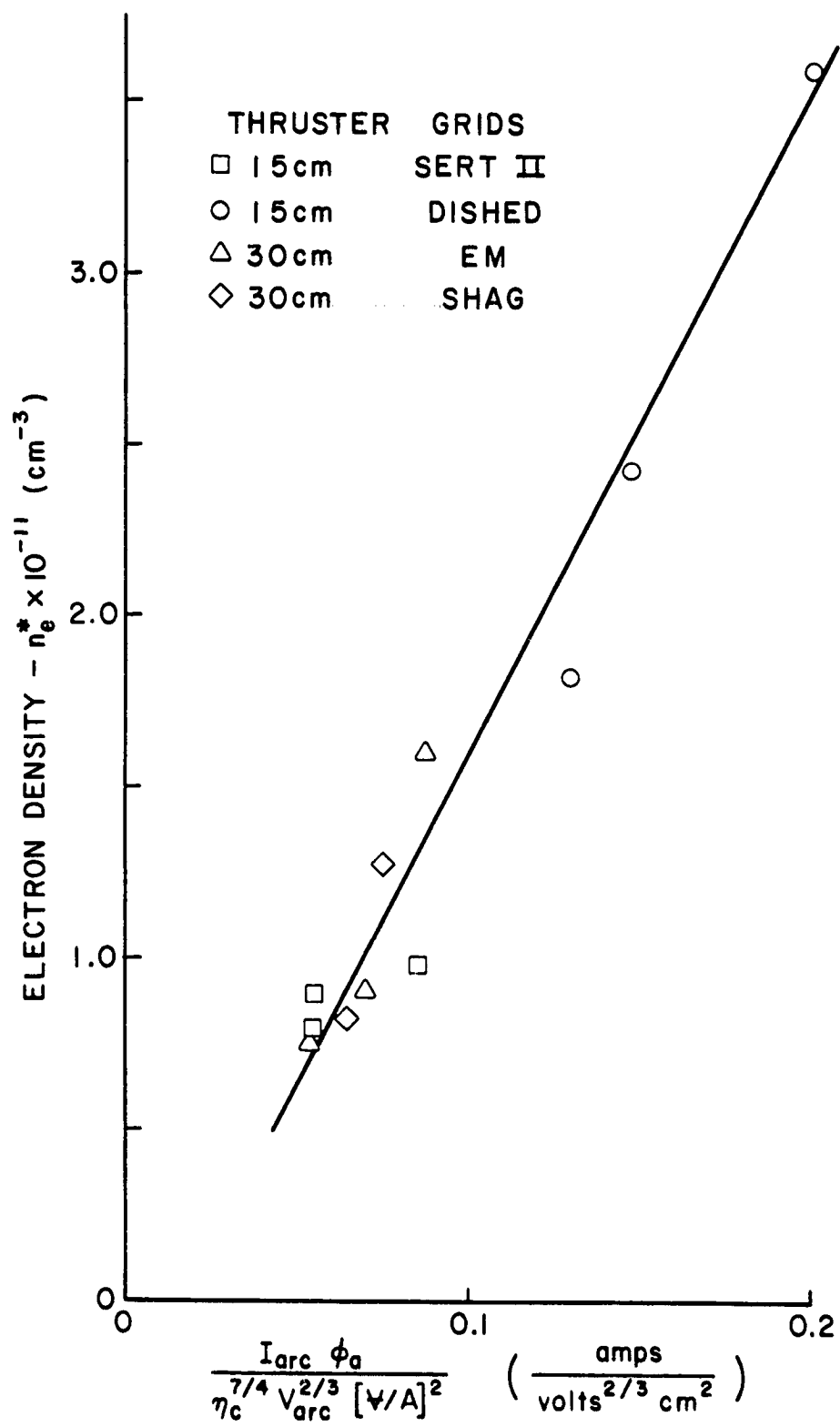


Figure 10 Electron Density Correlation

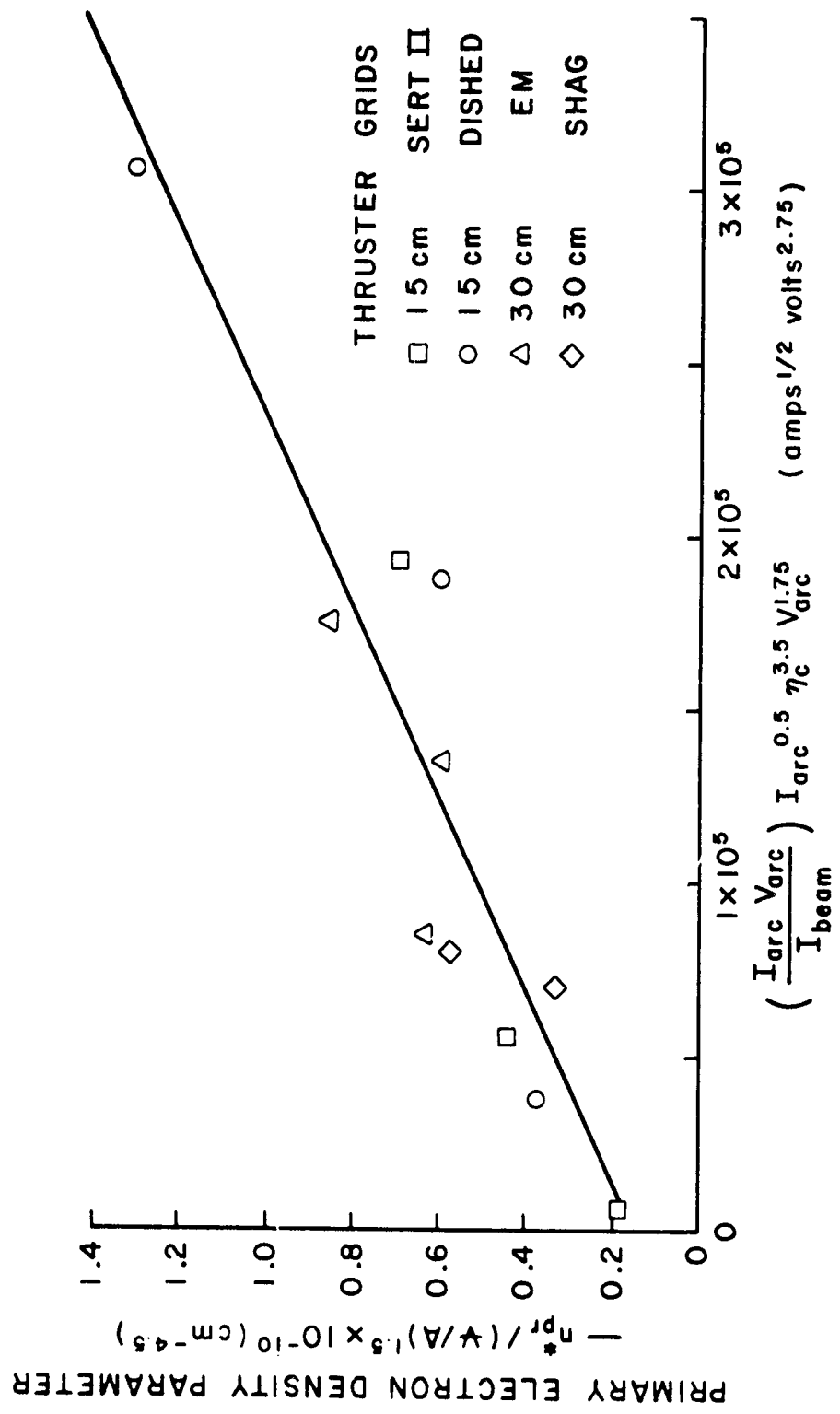


Figure 11 Primary Electron Density Correlation

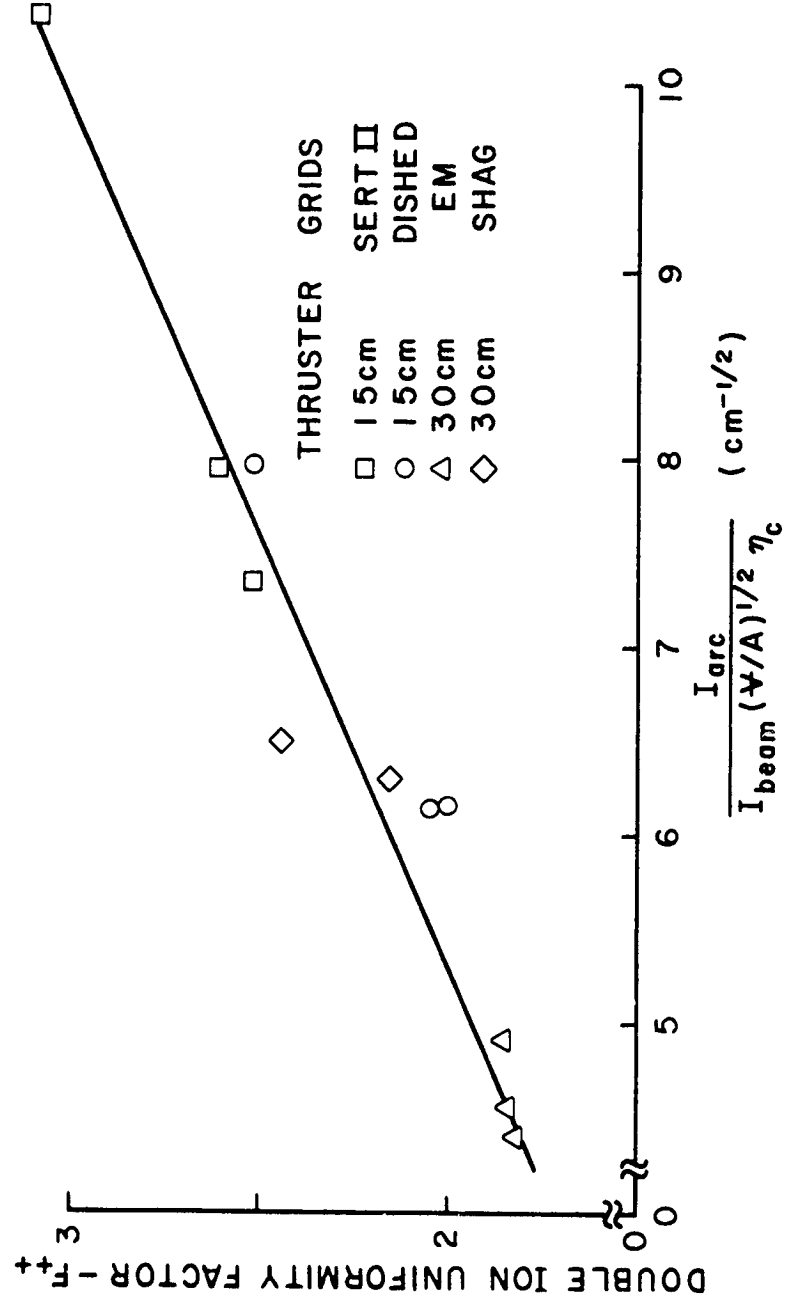


Figure 12 Uniformity Factor Correlation

Application of the simplified model can be best demonstrated through an example. Consider a 15 cm thruster operating at the conditions defined by the first section of Table IV. The corrected utilization (η_c) is first calculated using Equation (39) and a value of 68% is obtained. Next the correlating parameters are calculated. For example, the value of the correlating parameter

$$\left(\frac{I_{arc}}{I_{beam}} V_{arc} \right)^{.2} V_{arc}^{1/3} (\psi/A)^{-1/4}$$

used in Figure 8 is $8.3 \frac{\text{volts}}{\text{cm}^{1/4}}^{.533}$. This value indicates the average Maxwellian electron temperature would be 4.6 eV. The remainder of the average plasma properties were determined in a similar manner. The results obtained are listed in the second section of Table IV. Using the values of the primary electron energy and the Maxwellian electron temperature one can enter Figure 7 and determine $P_+^{++}(22 \text{ eV})$ and $Q_+^{++}(4.6 \text{ eV})$. These quantities, together with the average densities, the uniformity factor and the volume-to-surface area ratio for this thruster are then substituted into Equation (35) to obtain the double ion density as shown in the last section of Table IV. The double ion density calculated using the simplified model is $6.2 \times 10^1 \text{ cm}^{-3}$ while the value calculated using the complete model is $5.2 \times 10^1 \text{ cm}^{-3}$. The major reason for the discrepancy is that the electron temperature in Table IV (4.6 eV) is larger than the value used by the complete model (4.3 eV). This higher electron temperature causes $Q_+^{++}(T_{mx}^*)$ to be too large and results in the over-estimate of the double ion density.

Table IV.

Determination of the Double Ion Density Using the Simplified Model

Measured Thruster Variables

(15 cm Thruster)

$$\begin{array}{ll}
 I_{\text{arc}} = 3. \text{ amps} & \phi_s = .67 \\
 V_{\text{arc}} = 32.2 \text{ volt} & \phi_a = .67 \\
 I_{\text{beam}} = .499 \text{ amps} & V/A = 1.4 \text{ cm} \\
 n = .68 & \\
 n_c = .68 &
 \end{array}$$

Approximate Plasma Properties

$$\begin{array}{ll}
 T_{\text{mx}}^* = 4.6 \text{ eV} & n_{\text{pr}}^* = 4.64 \times 10^9 \text{ cm}^{-3} \\
 \varepsilon_{\text{pr}}^* = 22. \text{ eV} & n_e^* = 3.51 \times 10^{11} \text{ cm}^{-3} \\
 F_{++} = 2.55 & n_{\text{mx}}^* = n_e^* - n_{\text{pr}}^* = 3.46 \times 10^{11} \text{ cm}^{-3}
 \end{array}$$

Calculation of the Double Ion Density

$$\begin{aligned}
 n_{++}^* &= \frac{(3.51 \times 10^{11} \text{ cm}^{-3})^2 (1.4 \text{ cm}) (2.55)}{\left[9.6 \times 10^9 \frac{\text{cm}^2}{\text{sec}^2 \cdot \text{eV}} (4.6 \text{ eV}) (1.013) \right]^{\frac{1}{2}}} \\
 &\times \left[.013 (.55 \times 10^{-7} \frac{\text{cm}^3}{\text{sec}}) + .987 (.23 \times 10^{-8} \frac{\text{cm}^3}{\text{sec}}) \right] \\
 &= 6.2 \times 10^9 \text{ cm}^{-3}
 \end{aligned}$$

An examination of Equation (35) will indicate some general trends which should be considered in the design and operation of electron bombardment thrusters. For example, the double ion density varies linearly with the volume-to-surface area ratio. Therefore if two thrusters have the same average plasma properties the larger thruster will have a higher double ion density. Equation (35) suggests it would be desirable to reduce the electron density since the double ion density is proportional to the square of the electron density. However, making arbitrary adjustments in the plasma properties to reduce the double ion density may have an adverse effect on other aspects of thruster performance which must also be considered. An examination of the effect of electron density on propellant utilization will indicate one of the effects such an adjustment would have. The propellant utilization previously defined in Equation (36), is reproduced below.

$$\eta = 1 - \frac{n_{ot}^* v_o A_o / A_+}{n_+^* v_+} \quad (40)$$

The single ion density (n_+^*) can be approximated by the electron density (n_e^*). The total neutral density (n_{ot}^*) is the sum of the densities of all the neutral species and can be calculated using the equation

$$n_{ot}^* = n_o^* (1 + n_{int}^*/n_o^* + n_{rt}^*/n_o^*) \quad (41)$$

where n_{int}^* and n_{rt}^* are the total metastable and resonance states densities. The values of the ratios in Equation (41) can be calculated using equations similar in form to Equation (30). The neutral ground state density can be calculated using the equation

$$n_0^* = n_+^* (n_0^*/n_+^*) \approx n_e^* (n_0^*/n_+^*) \quad (42)$$

where the ratio (n_+^*/n_0^*) again takes a form similar to that of Equation (30). Combining these results into Equation (40) a result of the following form is obtained. "f" is a function of the Maxwellian electron temperature, primary electron energy, primary-to-Maxwellian electron density ratio and the uniformity factor F_+ . The dependence of the propellant utilization on the electron density and thruster parameters is explicitly shown.

$$\eta = 1 - \frac{A_0/A_+}{n_e^* A} f(T_{mx}^*, \varepsilon_{pr}^*, n_{pr}^*/n_{mx}^*, F_+) \quad (43)$$

One can see that a reduction in the electron density to reduce the double ion density will also have the undesirable effect of reducing the propellant utilization. However, if some changes in thruster design are made along with a reduction in the electron density the propellant utilization can be held constant while the double ion density is reduced. For example, if a new thruster were being designed one might double the volume-to-surface area ratio by making the thruster larger than its predecessor. It could then be operated at one-half the electron density of the predecessor allowing the propellant utilization to remain constant while exhibiting half the double ion density in accordance with Equation (35).

It might also be desirable to reduce the double ion density of a certain size thruster while maintaining the same propellant utilization. The propellant utilization could be held constant by reducing both the ratio A_0/A_+ (which reduces the relative escape rate of neutrals) and

the electron density in a manner that keeps the ratio $(A_0/A_+)/n_e^*$ constant. According to Equation (35) this would result in a large reduction in the double ion density which varies as the square of the electron density. The data in Table III for the two 30 cm thruster configurations at 1.5 and 2.0 amps beam current can be used to determine if theory and experiment agree for this method of double ion density reduction. The only difference in these two thruster configurations is the open area fraction of the accelerator grid. The EM accelerator grid has an open area fraction (ϕ_a) of 45% while the open area fraction for the SHAG accelerator grid is 23%. Both sets have a 69% open area fraction for the screen grid. The value of the ratio A_0/A_+ can be calculated for both grid sets using Equation (38). For the EM grids the ratio A_0/A_+ has a value of .39 while for the SHAG grids the value of the ratio is .25. The change from EM grids to SHAG grids then allowed operation at a given propellant utilization to occur at a lower arc voltage and hence a lower electron densities and energies and as a result lower double ion densities. In this particular case the double-to-single ion density ratios dropped from 4.4% and 6.0% to 2.2% and 2.8% respectively at two different utilizations when the SHAG grids were used. The theoretical model predicted essentially the same quantitative changes.

CONCLUSIONS

A discharge chamber model for an electron bombardment ion thruster has been developed which considers metastable, resonance and ground state atomic and ionic production and loss mechanisms. The model can be used to predict doubly charged ion densities from plasma property information. These calculated double ion densities agree with measured values to within 40% for low values of the double-to-single ion density ratio ($n_{++}/n_+ < 2\%$) and to within 20% for the rest of the data. Correlations, which relate average plasma properties to thruster operating variables such as anode current, can be used to estimate the average plasma properties in strongly divergent magnetic field thrusters when the properties themselves are not available. Singly charged ions are produced, according to this analysis, in significant numbers in two step processes through intermediate metastable and resonance states in addition to direct ionization from the neutral ground state. Doubly charged ions are produced predominantly via the singly ionized ground state with direct ground state neutral-to-double ion production becoming more significant in plasmas with high Maxwellian electron temperatures and primary electron energies. A simplified model which considers only the singly ionized ground state in double ion production can be used to predict double ion densities that agree with the complete model's predictions to within 5% when primary electron energies and Maxwellian electron temperatures are less than 29 eV and 5 eV respectively. The recent experimental observation⁽¹²⁾ that the use of small hole accelerator grids in conjunction with lower anode voltages provides a means for reducing double ion densities in thrusters, without degrading performance, is supported by the model.

REFERENCES

1. Kaufman, H. R., "Technology of Electron-Bombardment Ion Thrusters," Advances in Electronics and Electron Physics, Vol. 36, Academic Press, 1974.
2. Kieffer, L. J., "Electron Impact Ionization Cross Section Data for Atoms, Atomic Ions and Diatomic Molecules," Rev. Mod. Physics, Vol. 38, No. 1, pp. 15, 23, 1966.
3. Shpenik, O. B. and I. P. Azpesochnyi, "Excitation Cross Sections near the Threshold for Electron Atom Collisions," Optics and Spect., Vol. 23, pp. 7-10, 1967.
4. Kupriyanov, S. E. and Z. Z. Latypov, "Ionization of Positive Ions by Electrons," Soviet Physics JETP, Vol. 19, No. 3, pp. 558-559, Sept. 1964.
5. McConnell, J. C. and B. L. Moiseiwitsch, "Excitation of Mercury by Electrons," J. Phys. B., Vol. 1, No. 3, pp. 409-412.
6. Gryzinski, Michal, "Classical Theory of Atomic Collisions. I. Theory of Inelastic Collisions," Phys. Rev., Vol. 138, No. 2A, p. A341, April 19, 1965.
7. Strickfaden, W. B. and K. L. Geiler, "Probe Measurements of the Discharge in an Operating Electron Bombardment Engine," AIAA Journal, Vol. 1, No. 8, pp. 1815-1823, August 1963.
8. Masek, T. D., "Plasma Properties and Performance of Mercury Ion Thrusters," AIAA Paper No. 69-256, March 3-5, 1969.
9. Wilbur, P. J., "Hollow Cathode Restartable 15 cm Diameter Ion Thruster," NASA CR-134532, December, 1973.
10. Peters, R. R. and P. J. Wilbur, "Double Ion Production in Mercury Thrusters," AIAA Paper 75-398, March 19-21, 1975.
11. Mitchell, A. C. G., 'Resonance Radiation and Excited Atoms,' Cambridge at the University Press, 1961.
12. Vahrenkamp, R. P., Personal Communication, January, 1976.
13. Bechtel, R. J., Csiky, G. A., and D. C. Byers, "Performance of a 15-centimeter Diameter, Hollow Cathode Kaufman Thruster," AIAA Paper No. 68-88, January 22-24, 1968.
14. Poeschel, R. L., King, H. J., and D. E. Schneider, "An Engineering Model 30 cm Thruster," AIAA Paper No. 73-1084, Oct. 31 - Nov. 2, 1973.

15. Poeschel, R. L., et al., "2.5 Kw Advanced Technology Ion Thruster," NASA CR-134687, August, 1974.
16. Poeschel, R. L., et al., "High Power and 2.5 Kw Advanced Technology Ion Thruster," Monthly Report No. 7, Contract NAS 3-19703, January, 1976.
17. Wilbur, P. J., "15 cm Diameter Ion Thruster Research," NASA CR-134755, December, 1974.
18. Wilbur, P. J., "An Experimental Investigation of a Hollow Cathode Discharge," NASA CR-130847, December, 1971.
19. Vahrenkamp, R. P., "Measurement of Doubly Charged Ions in the Beam of a 30 cm Mercury Bombardment Thruster," AIAA Paper No. 73-1057, Oct. 31 - Nov. 2, 1973.
20. Wilbur, P. J., "15 cm Mercury Ion Thruster Research," NASA CR-134905, December, 1975.

APPENDIX A

The computer program "HG", which can be used to predict the densities of excited atomic and ion states considered in the complete model, is listed below. The input parameters needed by this program can be approximated using the correlations in Figures 8-12. More accurate input parameters can be determined using the computer program "PROP", listed in Appendix B, and data obtained from a Langmuir probe survey of the discharge chamber. The computer program "HG" uses the equations developed in the "Theoretical Model" section and carrys out the calculations in the manner suggested at the end of that section. Comment cards are included in the listing to indicate what calculations, etc. are to be carried in each section.

Values of the functions $P_{\alpha}^{\gamma}(\xi_{pr})$ and $Q_{\alpha}^{\gamma}(T_{mx})$ are listed immediately after the computer program listing. The particular initial state (α) and final state (γ) are indicated in the last twenty columns. For example, the label "HGM-HG+ 3P0" indicates the initial state for the reaction is the 6^3P_0 metastable state and the final state is the singly ionized ground state. The first seven cards listed with a particular identifying label contain the values for $P_{\alpha}^{\gamma}(\xi_{pr})$ while the second seven list values for $Q_{\alpha}^{\gamma}(T_{mx})$.

```

PROGRAM HG (INPUT,OUTPUT,PUNCH,TAPES=INPUT,TAHF6=OUTPUT,TAPE8=PUNCHG . 10
1H,F11MPL)
COMMON /A/ NP,NM,TEMP,PRINRG
COMMON /R/ UTT(4,25),PD(4,25),IK
DIMENSION A(8), R(3), C(3), D(3), F(3), SX00M(2,2,21), SE00M(2,2,2HG
11), SX01(2,21), SE01(2,21), SX02(2,21), SE02(2,21), SX0M1(2,2,21), HG
2 SE0M1(2,2,21), SX11M(2,2,21), SF11M(2,2,21), SX12(2,21), SE12(2,2HG
31), RR(2), TR(2), SE1N2(2,2,21), RA0M0(2), RA1M0(2), SX(2,21), SF(HG
42,21), P2(B), TI(B), X(8), Y(B), G(B), R(5), Z(B), H(B), SX0R(2,2,HG
521), SF0R(2,2,21), SF1R(2,2,21), FR(2), TM(2), W(2), HG 100
6 G(2), TK(2), XSM(2), XSM(2), XPSMM(2), FREE(2), PHLOSS(MG
721), TAU(2), XLAM(2), OPP(6,6), XNF(6), XL(3,6,10), PNE(6,10), SP(6HG
8,6), PEA(7), HA(7), PYP(30), PNO(4), SN(14,6,10), TT1(14,8), PP(10HG
9), PR(10), FXP(30), SX1M2(2,2,21), TMP(5), QT(B), QR(B) 140
REAL NP,NM
DATA X(1),TTI(1,1),TTI(2,1),TTI(3,1),TTI(4,1),TTI(5,1),TTI(6,1),TTHG
11(7,1),TTI(8,1),TTI(9,1),TTI(10,1),TTI(11,1),TTI(12,1),TTI(13,1),THG
2TI(14,1),TM,TR,TK,H(1),Z(1),Z(2)/10HPRI ENRGY,10HNEUT DENS,,10HNMGHG
3/N0 PERC,10HNK/N0 PFHC,10HN+/N0 PERC,10HNH+/N0 PE,,10HN++/N0 PFH,1HG
40HN+/NOT ,10HN++/NOT ,10HREAM MA. ,10HN+ CM-3 ,10HN++ CM-3HG
5 ,10HI ARC AMP,,10-EV/BFAION,10H ,10HA 3P0 ,10H6 3PHG
62 ,10HA 3P1 ,10HA 1P1 ,10H6 2D 5/2 ,10H6 2D 3/2 ,10HHG
7N++/N+ ,10HPLOT WITH ,10HM CONSTANT/ 220
DATA EP,TAU,XLAM/5.545+6.7,.000000010H,.0000000013,.00002537,.00001HG
1849/
FR(A,B)=(A(1)*R(1)+A(2)*R(2))/(A(1)+A(2)) 250
HG 260
HG 270
HG 280
HG 290
HG 300
HG 310
HG 320
HG 330
HG 340
HG 350
HG 360
HG 370
HG 380
HG 390
HG 400
HG 410
HG 420
HG 430
HG 440
HG 450
HG 460
HG 470
HG 480
HG 490
HG 500
HG 510
HG 520
HG 530
HG 540
HG 550
HG 560
HG 570
HG 580
HG 590
HG 600
HG 610
HG 620
HG 630
HG 640
HG 650
C THIS PROGRAM IS SET UP FOR MERCURY ONLY
C SET UP OF THE PROGRAM
C
NMZ=10
NNN=0
DC 101 I=2+8
    H(I)=10H
101 X(I)=10H
DO 102 I=3+8
    H(I)=10H
102 Z(I)=10H
DO 103 J=1+14
    DO 103 I=2+8
    H(I)=10H
103 TTI(J,I)=10H
DO 104 I=1+8
    QT(I)=TTI(13,I)
104 QR(I)=10H
QR(1)=10HUTL.
NU=2
DO 105 I=1+3
    A(I)=1.
105 A(I)=1.
C READ IN THE INTEGRATED CROSS SECTIONS
C 1 -- INDICATES DATA FOR PRIMARY ELECTRONS
C 2-- INDICATES DATA FOR MAXWELLIAN ELECTRONS
C
C NEUTRAL TO SINGLE
C
C READ (5,16B) ((SF01(J,I),SX01(J,I),I=1,21),J=1,2)
C
C NEUTRAL TO DOUBLE
C
C READ (5,16B) ((SF02(J,I),SX02(J,I),I=1,21),J=1,2)
C
C SINGLE TO DOUBLE
C
C READ (5,16B) ((SF12(J,I),SX12(J,I),I=1,21),J=1,2)
C
C NEUTRAL TO METASTABLE

```

```

C READ (5,168) (((SE00M(I,J,K),SX00M(I,J,K),K=1,21),J=1,2),I=1,2) HG 560
C NEUTRAL TO RESONANCE HG 670
C READ (5,168) (((SE01P(I,J,K),SX01P(I,J,K),K=1,21),J=1,2),I=1,2) HG 680
C METASTABLE ATOM TO SINGLE HG 690
C READ (5,168) (((SE01M(I,J,K),SX01M(I,J,K),K=1,21),J=1,2),I=1,2) HG 700
C SINGLE METASTABLE TO DOUBLE HG 710
C READ (5,168) (((SE1M2(I,J,K),SX1M2(I,J,K),K=1,21),J=1,2),I=1,2) HG 720
C RESONANCE TO SINGLE HG 730
C READ (5,168) (((SE1R1(I,J,K),SX1R1(I,J,K),K=1,21),J=1,2),I=1,2) HG 740
C SINGLE TO SINGLE METASTABLE HG 750
C READ (5,168) (((SE11M(I,J,K),SX11M(I,J,K),K=1,21),J=1,2),I=1,2) HG 760
C READ IN DATA HG 770
C ND-NO. OF DIFFERENT PRIMARY ENERGIES DESIRED FOR EACH ELECTRON DEN HG 780
C DP-( BELOW) DELTA PRIMARY ENERGY HG 790
C NS-NO. OF DIFFERENT ELECTRON DENSITIES USED PER RUN HG 800
C MHR-NO. OF RUNS HG 810
C IFLAG=1 NO INTERPOLATION FOR MASS FLOW RATE HG 820
C READ (5,142) ND,NS,MHR,IFLAG HG 830
C BEGIN THE RUNS HG 840
C DP=10. HG 850
C DO 13H IP=1,MHR HG 860
C EQUIVALENT OPEN AREA FOR NEUTRALS AND CHARGED PARTICLES, VOLUME OF HG 870
C PRIMARY ELECTRON REGION, NONUNIFORMITY PARAMETERS. HG 880
C READ (5,141) DPN,DMC,VOL,F1,F2 HG 890
C NO. OF DIFFERENT MASS FLOW RATES DESIRED HG 900
C NCF=2 HG 910
C VALUES OF M HG 920
C IF (IFLAG,FC,1) GO TO 106 HG 930
C READ (5,141) (PFD(I),I=1,NCF) HG 940
C KKK=1 HG 950
C XNT=.05 HG 960
C DO 129 J=KKK,NS HG 970
C PFD(J)=15. HG 980
C XAL=.05 HG 990
C XM=.0. HG 1000
C XZ=.0. HG 1010
C 106 HG 1020
C PRIMARY ELECTRON VELOCITY TO AREA, MAX. TEMPERATURE, DUMMY, PRIMARY ZHG 1030
C MAXWELLIAN PARTITION, ELECTRON DENSITY. HG 1040
C READ (5,141) (A,TEMP,DUMMY,ND,DELTAS) HG 1050
C IF (CTFL,FC,1) GO TO 107 HG 1060
C READ (5,141) (A,TEMP,DUMMY,ND,DELTAS) HG 1070
C IF (CTFL,FC,1) GO TO 108 HG 1080
C IF (CTFL,FC,1) GO TO 109 HG 1090

```

```

C      ELECTRON DENSITIES FOR ITERATION ON MASS FLOW RATE      HG 1320
C
C      READ (5,140) (TMP(L),L=1,NS)      HG 1330
C      GO TO 109      HG 1340
107    ELDENS=TMP(JJ)      HG 1350
C      GO TO 109      HG 1360
108    WRTTF (5+139)      HG 1370
C      CONTINUE      HG 1380
109    XNF(JJ)=ELDENS      HG 1390
C      ELD=ELDENS/1.F18      HG 1400
C      ENCODE (64,144,II) VA,ELD,TEMP,DENR      HG 1410
C      DO 128 II=1,ND      HG 1420
C          SEV=0.
C          WRITE (6,145) VA,ELDENS,TEMP,PHINP,DENR      HG 1430
C          WRITE (6,146) VOL,OPN,OPC,F1,F2      HG 1440
C          TOT=1.+1./DENR      HG 1450
C          NP=ELDENS/TOT      HG 1460
C          NM=ELDENS/TOT/DENR      HG 1470
C          FFNL=20.*TEMP      HG 1480
C          CALL YINTEG (SX02,SE02,1.,SUMM,PRSUMM)      HG 1490
C
C      CALCULATION OF METASTABLE/ NEUTRAL GROUND STATE RATIO      HG 1500
C
C      DO 112 J=1,2      HG 1510
C          DO 110 I=1,2      HG 1520
C              DO 110 K=1,21      HG 1530
C                  SX(I,K)=SX00M(J,I,K)      HG 1540
110    SE(I,K)=SE00M(J,I,K)      HG 1550
C                  CALL YINTEG (SX,SE,1.,SUM,PRSUM)      HG 1560
C              DO 111 I=1,2      HG 1570
C                  DO 111 K=1,21      HG 1580
C                      SX(I,K)=SX0M1(J,I,K)      HG 1590
111    SE(I,K)=SE0M1(J,I,K)      HG 1600
C                  CALL YINTEG (SX,SE,1.,SUM2,PRSUM2)      HG 1610
C                  WLOSS=230./VA/4.      HG 1620
C                  WALL=WLOSS      HG 1630
C                  RAOM0(J)=SUM/(WLOSS+SUM2+SUMM)      HG 1640
C                  WRITE (6,147) TM(J),RAOM0(J)      HG 1650
C                  WRITE (6,161)      HG 1660
C                  WRITE (6,163) SUM,PRSUM      HG 1670
C                  SEV=SEV+SUM*PRSUM      HG 1680
C                  WRITE (6,162)      HG 1690
C                  WRITE (6,167) WLOSS,SUM2,PRSUM2,SUMM,PRSUMM      HG 1700
C                  TT=WLOSS+SUM2+SUMM      HG 1710
C                  AA=WLOSS/TT      HG 1720
C                  AB=SUM2/TT      HG 1730
C                  AC=SUMM/TT      HG 1740
C                  WRITE (6,148) AA,AB,AC      HG 1750
112    CONTINUE      HG 1760
C                  SD(2,JJ,II)=(RAOM0(1)+RAOM0(2))^100.      HG 1770
C
C      CALCULATION AND ITERATION FOR RESONANCE/NEUTRAL, SINGLE/NEUTRAL, +HG 1780
C      NEUTRAL DENSITY      HG 1790
C
C          JKLE=-1      HG 1800
C          IFLAG=0      HG 1810
C          IZ=II-2      HG 1820
C          II=II-1      HG 1830
C          IF (II.GT.2) XN1=(2.*SD(4,JJ,II)-SD(4,JJ,II))/100.      HG 1840
C          XN1=XN1+XNM+XN2      HG 1850
C          XSM(2)=0.      HG 1860
C
C      GUESS NEUTRAL DENSITY      HG 1870
C
C          XNO=ELDENS*IT/1000000.      HG 1880
113

```

```

C      CALCULATE RESONANCE/NEUTRAL RATIO          HG 1980
C
C      DO 117 J=1,NQ
C      IF (IFLAG,FQ,1) GO TO 116                  HG 1990
C      DO 114 I=1,2                                HG 2000
C      DO 114 K=1,2                                HG 2010
C      SX(I,K)=SX0R(J,I,K)                         HG 2020
C      SE(I,K)=SE0R(J,I,K)                         HG 2030
C      CALL YINTEG (SX+SE+1.,XSM(J),XPSN(J))      HG 2040
C      DO 115 I=1,2                                HG 2050
C      DO 115 K=1,2                                HG 2060
C      SX(I,K)=SXRI(J,I,K)                         HG 2070
C      SE(I,K)=SER1(J,I,K)                         HG 2080
C      CALL YINTEG (SX+SE+1.,XSM(J),XPSM(J))       HG 2090
C      116  CONTINUE                                 HG 2100
C      DVO=33963./XLAM(J)                          HG 2110
C      SIGMAC=.112/DVO*XLAM(J)**2/TAU(J)           HG 2120
C      FREE(J)=1./((XNO*SIGMAC)                   HG 2130
C      PHLOSS(J)=1./((9.E12*VA*(TAU(J)*XNO*SIGMAC)**2) HG 2140
C      RR(J)=XSM(J)/(WALL+PHLOSS(J)+XSM(J)+SUMM)   HG 2150
C      IF (IFLAG,FQ,1) GO TO 118                  HG 2160
C      CALL YINTEG (SX01,SE01+1.,SUM1,PRSUM1)        HG 2170
C      CALL SUMIT (SX01,SE01,2,RAOM0,TSUM1,B,C)      HG 2180
C      *(?)=0.                                     HG 2190
C      Q(?)=0.                                     HG 2200
C      118  CALL SUMIT (SXRI,SER1,NQ,RR,TSS,W,Q)    HG 2210
C      IF (IFLAG,FQ,1) GO TO 119                  HG 2220
C
C      CALCULATION OF SINGLE/NEUTRAL RATIO          HG 2230
C
C      VP=SQRT(TEMP**4,8038E9*(1.+NP/NM))/100.     HG 2240
C      WLLOSS=VP/VA/F1                             HG 2250
C      CALL SUATT (SX11M,SE11M,2+A+TSUM2,D,E)       HG 2260
C      CALL YINTEG (SX12,SE12,1.,SUM2,PRSUM2)        HG 2270
C      RNTO=(SUM1+TSUM1+TSS)/(WLLOSS+TSUM2+SUM2)    HG 2280
C
C      CHECK OF ERROR IN GUESS OF NEUTRAL DENSITY   HG 2290
C
C      RNPO=RN10+XN2+XNM                           HG 2300
C      ERROK=ABS((RNPO-XN1)/RNPO)                  HG 2310
C      XN1=XN10+XN2+XNM                           HG 2320
C      XN1=XN10                                     HG 2330
C      JK1=JKL+1                                    HG 2340
C      JK1=JKL+1                                    HG 2350
C      IFLAG=1                                     HG 2360
C      IF (ERROR.GT.,03) GO TO 113                 HG 2370
C
C      NEUTRAL GROUND STATE ATOM DENSITY             HG 2380
C
C      XNO=EDENS/XN1/1000000.                      HG 2390
C      WRITE (6,144) XN1,JKL                        HG 2400
C      SD(3,J,J+1)=RR(1)+RR(2)+100.                HG 2410
C      SD(1,J,J+1)=XNO                            HG 2420
C      SD(4,J,J+1)=XNO*100.                         HG 2430
C      XKA=100.0/(100.+SD(1,J,J+1)+SD(2,J,J+1))  HG 2440
C      SD(7,J,J+1)=XKA*100.                         HG 2450
C      XNT=XNO*(1.+RAOM0(1)+RAOM0(2)+RR(1)+RR(2)) HG 2460
C      XL(1,J,J+1)=XNT/5750.                        HG 2470
C
C      PRINT OUT RESONANCE ATOM DENSITY RATIO       HG 2480
C
C      DO 170 J=1,NQ
C      WRITE (6,145) TKE(J)+PKE(J)+FREE(J)        HG 2490
C      WRITE (6,161)
C      WRITE (6,163) XS1(J)+XPRI(J)
C      WRITE (6,164) XPSN(J)
C      WRITE (6,162) HG 2500

```

```

      1      WRITE (6,152) WALL+PHLOSS(J)+XSMM(J)+XPSMM(J),SUMM,PRSHG 2640
      1      (SUMM
      1      TT=WALL+PHLOSS(J)+XSMM(J)+SUMM               HG 2650
      1      AA=WALL/TT                                HG 2660
      1      AH=XSMM(J)/TT                            HG 2670
      1      AC=SUMM/TT                                HG 2680
      1      AD=PHLOSS(J)/TT                            HG 2690
      1      WRITE (6,151) AA,AD,AH,AC                HG 2700
      120    CONTINUE                                  HG 2710
      C      PRINT OUT SINGLE ION DENSITY RATIO          HG 2720
      C
      C      WRITE (6,153) RN10                         HG 2730
      C      SD(10,JJ,II)=RN10*XNO                      HG 2740
      C      PRIF=FR(B,C)                            HG 2750
      C      WRITE (6,161)                           HG 2760
      C      PRIG=FR(W,D)
      C      PRIH=FR(D,E)
      C      WRITE (6,164) SUM1,PRSUM1,TSUM1,PRIF,TSS,PRIG 2770
      C      SEV=SFV+SUM1*PRSUM1+TSUM1*PRIF+TSS*PRIG
      C      TT=SUM1+TSUM1+TSS
      C      AA=SUM1/TT                                HG 2780
      C      AB=TSUM1/TT                                HG 2790
      C      AC=TSS/TT                                 HG 2800
      C      WRITE (6,154) AA,AB,AC                     HG 2810
      C      WRITE (6,162)                           HG 2820
      C      WRITE (6,167) WLOSS,SUM2,PRSUM2,TSUM2,PRIH 2830
      C      TT=SUM2+WLOSS+TSUM2
      C      AA=WLOSS/TT                                HG 2840
      C      AB=SUM2/TT                                HG 2850
      C      AC=TSUM2/TT                                HG 2860
      C      WRITE (6,148) AA,AB,AC                     HG 2870
      C
      C      CALCULATION OF SINGLE METAL/NEUTRAL RATIO   HG 2880
      C
      C      DO 123 J=1,2                               HG 2990
      C      DO 121 I=1,2                               HG 3000
      C      DO 121 K=1,21                             HG 3010
      C      SX(I,K)=SX1IM(J,I,K)                      HG 3020
      C      121     SE(I,K)=SE1IM(J,I,K)                HG 3030
      C      CALL YINTEG (SX,SE,RN10,SUM1,PRSUM1)        HG 3040
      C      DO 122 I=1,2                               HG 3050
      C      DO 122 K=1,21                             HG 3060
      C      SX(I,K)=SX1M2(J,I,K)                      HG 3070
      C      SE(I,K)=SE1M2(J,I,K)                      HG 3080
      C      122     CALL YINTEG (SX,SE,1.,SUM2,PRSUM2)  HG 3090
      C      WLOSS=VP/VA/F2                            HG 3100
      C      RA1MO(J)=SUM1/(SUM2+WLOSS)                HG 3110
      C      WRITE (6,155) TK(J),RA1MO(J)              HG 3120
      C      WRITE (6,161)                           HG 3130
      C      WRITE (6,163) SUM1,PRSUM1                 HG 3140
      C      SEV=SFV+SUM1*PRSUM1
      C      WRITE (6,162)                           HG 3150
      C      WRITE (6,166) WLOSS,SUM2,PRSUM2           HG 3160
      C      TT=WLOSS+SUM2
      C      AA=WLOSS/TT                                HG 3170
      C      AB=SUM2/TT                                HG 3180
      C      WRITE (6,148) AA,AB                     HG 3190
      C
      123    CONTINUE                                  HG 3200
      C      X1(2,J,I,II)=(RN10*RA1MO(1)+RA1MC(2))/VP*XNO*100.
      C      XNM=RA1MO(1)*RA1MO(2)                      HG 3210
      C      IF ((I,I,GT,1) XNM=2.*XNM=SD(S,J,I,II)/100.  HG 3220
      C
      C      CALCULATION OF DOUBLE/NEUTRAL RATIO          HG 3230
      C
      C      CALL YINTEG (SD,O2,SD,O2+1.,SUM1,PRSUM1)  HG 3240
      C

```

```

CALL YINTEG (5+12+SE12P,RA10,PRSUM1,PRSUM2)
CALL SUMIT (SX1M2+SE1M2+2,RA1M0,TSUM1,B,C)
WLOSS=1.41428VP/VA/F2
RK=0.
SD(5+JJ+II)=(RA1M0(1)+RA1M0(2))*100.
DO 124 I=1,2
RK=RK+RA0M0(I)*SUMM
RL=0.
DO 125 I=1,NG
RL=RL+R(I)*SUMM
R20=(SUM1+SUM2+TSUM1+RK+RL)/WLOSS

C PREDICTION OF NEXT DOUBLE ION/NEUTRAL FOR USE IN PREDICTION
C OF NEUTRAL DENSITY
C
IF (II.EQ.1) GO TO 126
II=II-1
XN2=(2.*R20-SD(5+JJ+II)*.01)*2.
GO TO 127
126 XN2=2.*R20
CONTINUE
SD(11+JJ+II)=R20*XN0
SD(2+JJ+II)=R20*XXA
XL(3+JJ+II)=R20*VP*1.41428*XN0*100.
SD(6+JJ+II)=R20*100.

C WRITE DOUBLE/NEUTRAL RATIO, ETC.
C
WRITE (6+156) R20
G(I)=PRINTG
PN=FR(B,C)
WRITE (6+161)
WRITE (6+165) SUM1+PRSUM1,SUM2+PRSUM2+TSUM1,PN,RK,PRSUMM
SEV=SEV+SUM1*PN+(1.+SUM2+PRSUM2+TSUM1)*PN+(RK+RL)+PRSUMM
TT=SUM1+SUM2+TSUM1+RK+RL
AA=SUM1/TT
AB=SUM2/TT
AC=TSUM1/TT
AD=RK/TT
AE=RL/TT
WRITE (6+157) AA,AB,AC,AD
WRITE (6+153) XL+PRSUMM
WRITE (6+158) AE
WRITE (6+152)
WRITE (6+156) WLOSS

C BEAM CURRENT
C
XXXX=(XL(2+JJ+II)+XL(3+JJ+II)*2.)*1.6E-16*OPC
C MASS LOSS RATE
C
TOTLOSS=(XL(1+JJ+II)*OPC+(XL(2+JJ+II)+XL(3+JJ+II))*OPC)*1E9
1 .6E-16
TOTLOSS=XXXX/TOTLOSS
TOTLOSS=1E-16*TOTLOSS

C EMISSION
C
EV=1.6E-16*XXXX*1.6E-16*OPC*VCL
C ABC CURRENT
C
ABC=1.6E-16*XXXX*1.6E-16*OPC*VCL
ABC=1.6E-16*ABC
ABC=1.6E-16*ABC

```

```

      WRITE (6,159) XXXX,UTL,FV,ARCI          HG 3960
C
C      CHECK FOR PLASMA NEUTRALITY             HG 3970
C
C      EP=ABS((XNM+XN2+RN10)/XNI-1.)
C      IF (IFLAG,FI,1,AND,EP,GT,.03) GO TO 108   HG 3980
C      PRINNG=PRINRG+DP                         HG 3990
C      IF (IFLAG,NE,0) GO TO 138                 HG 4000
128      CONTINUE                               HG 4010
129      CONTINUE                               HG 4020
C
C      INTERPOLATION FOR THE ELECTRON DENSITY WHICH YIELDS DESIRED MASS   HG 4030
C      LOSS RATE                                HG 4040
C
C      DO 132 IY=1,NS                          HG 4050
C
C      LOSS RATE                                HG 4060
C
C      DO 131 JZ=1,ND                          HG 4070
C      DO 130 JY=1,NS                          HG 4080
C          PYP(JY)=(XL(1,IY,JZ)*OPN+(XL(2,IY,JZ)+XL(3,IY,JZ))*OPCHG 4090
C          )*1.6F-16                           HG 4100
1            CONTINUE                               HG 4110
130      CONTINUE                               HG 4120
C      WRITE (6,160) (PYP(JK),JK=1,NS)           HG 4130
C      DO 131 JA=1,NC                          HG 4140
C          CALL AITKEM (PYP+XNF,NS+2,PN0)(JA),PNE(JA,JZ)) 4150
C          IF (PNE(JA,JZ).LT.0.) PNE(JA,JZ)=0.               HG 4160
131      CONTINUE                               HG 4170
C
C      CALCULATE N++/N+                          HG 4180
C
C      DO 132 IZ=1,ND                          HG 4190
C          OPP(IY,IZ)=SD(h,IY,IZ)/SU(4,IY,IZ)           HG 4200
132      CONTINUE                               HG 4210
C          CALL CRSPLT (PN0,OPP,XNE,PNE,G,X,Y,Z,ND,NS,NC) 4220
C
C      INTERPPOLATION OF PLASMA PROPERTIES ETC. FOR CONSTANT MASS LOSS RATHG 4230
C
C      DO 135 IK=1,13                          HG 4240
C          DO 133 IF=1,8                        HG 4250
133      Y(IF)=TTI(IK,IF)                     HG 4260
C          DO 134 IE=1,NS                      HG 4270
C          DO 134 IF=1,ND                      HG 4280
134      OPP(IF,IF)=SD(IK,IE,IF)           HG 4290
C          CALL CRSPLT (PN0,OPP,XNE,PNE,G,X,Y,Z,ND,NS,NC) 4300
HG 4310
C
C      CONTINUE                               HG 4320
C
C      DO 137 L=1,NC                          HG 4330
C          DO 136 K=1,25                      HG 4340
C              PXP(K)=UTT(L,K)/PN0(L)           HG 4350
136      PYP(K)=PD(L,K)                     HG 4360
C          CALL MAPA (5,PXP,PYP+1,25,HL,HH,VL,VH,QR,QT,Z,1) 4370
137      CALL MAPM (5,PXP,PYP+1,25,HL,HH,VL,VH,QR,QT,Z,1) 4380
138      CONTINUE                               HG 4390
C
C      139 FORMAT (2X,16HITERATION FOR N+)        HG 4400
140      FORMAT (AF10.4)                      HG 4410
141      FORMAT (AF10.4)                      HG 4420
142      FORMAT (16I4)                        HG 4430
143      FORMAT (4F10.4,F10.2)                HG 4440
144      FORMAT (4HV/A=,F6.3,9X,3HEDE,F6.3,3HE18,9X,2HT=+F4.1,9X,4HV/H=,F5, 4450
145      12)                                  HG 4460
145      FORMAT (//,3X,14HVOL XAHFA(M+1)= ,1.4,5X,14HEFLC UFN(M-3)=F11.4,5HG 4470
1X,14HEFLC TEMP(EV)=+F7.3,5X,16F-P-L, ENERGY(EV)=+F7.3,5X,6HNPD/NM=,FHG 4480
26.5)                                 HG 4490
146      FORMAT (/10X,10HVOL (CA3)=,F10.3,10X,7HA-NFHUT=,F10.3,10X,10HA-- (HG 4500
1CM2)=,F10.3,3X, 3HF1=,F6.2,3X, 3HF2=,F6.2)           HG 4510

```

```

147 FORMAT (//,20X,A10,5X,4HNMETA/NO=.F10.5) HG 4620
148 FORMAT (10X,F10.5,21X,2(F10.5,20X)) HG 4630
149 FORMAT (/,10X,23HNEUTRAL DENSITY (CM-3)=,E10.3,10X,15HNO. ITERATING HG 4640
  IONS=,I4) HG 4650
150 FORMAT (//,20X,A10,5X,8HNHFS/NO=.F10.6,10X,20HMEAN FREE PATH (CM)=HG 4660
  1,F8.5) HG 4670
151 FORMAT (11X,F10.5,20X,3(F10.5,20X)) HG 4680
152 FORMAT (10X,F11.4,20X,F11.4,20X,2(E11.4,1X,E9.2,10X)) HG 4690
153 FORMAT (//,20X,6HN+/NO=.F10.5) HG 4700
154 FORMAT (10X,3(F10.5,20X)) HG 4710
155 FORMAT (//,20X,A10,5X,1UHN+META/NO=.F10.5) HG 4720
156 FORMAT (//,20X,7HN+/NO=.F10.5) HG 4730
157 FORMAT (10X,4(F10.5,21X),/) HG 4740
158 FORMAT (10X,F10.5) HG 4750
159 FORMAT (/,5X,5HREAM=.F10.3,3HMA.,10X,12HUTILIZATION=.F10.6,10X,16HHG 4760
  1EV PER RFAM ION=.F10.5,10X,5HIARC=.F10.3) HG 4770
160 FORMAT (/.2X,3HM/A,8(3X,F10.1)) HG 4780
161 FORMAT (/,20X,49HNUMERATOR TERMS (1/SEC) FOLLOWED BY PRI. FRACTIONHG 4790
  1) HG 4800
162 FORMAT (/,20X,52HDENOMINATOR TERMS FOLLOWED BY PRI. FRACTION (IF AHG 4810
  1NY)) HG 4820
163 FORMAT (10X,F11.4,1X,E9.2) HG 4830
164 FORMAT (10X,3(F11.4,1X,E9.2,10X)) HG 4840
165 FORMAT (10X,4(F11.4,1X,E9.2,10X)) HG 4850
166 FORMAT (10X,F11.4,20X,F11.4,1X,E9.2,10X) HG 4860
167 FORMAT (10X,F11.4,20X,2(F11.4,1X,E9.2,10X)) HG 4870
168 FORMAT (3(F10.4,F10.3),20X) HG 4880
HG 4890
HG 4900

C
  END

SUBROUTINE CRSPLT (PNO,UPP,XNE,PNE,G,X,M,Z,ND,NS,NC) CRS 10
C
C THIS SUBROUTINE INTERPOLATES IN THE ARRAY DPP TO GET THE VALUES FOR CRS 30
C CONSTANT MASS FLOW RATE (DET. BY PNE) AND THEN PLOTS THE RESULTS CRS 40
C
C COMMON /R/ UTL(4,25)*PD(4,25)*IK CRS 50
C DIMENSION DPP(6,6), PNO(4), XNF(6), PMF(6,10), G(8), PYP(30), PXP(CRS 70
C 130), PP(30), SP(10,30), X(8), Y(8), H(M), /4/ CRS 80
C
C INTERPOLATION CRS 90
C
C DO 102 KZ=1,ND CRS 100
C   DO 101 KY=1,NS CRS 110
101   PYP(KY)=DPP(KY,KZ) CRS 120
C   DO 102 KX=1,NC CRS 130
C     CALL AJTKFN (XNE,PYP,NS,2,PNE(KX,KZ),SP(KX,KZ)) CRS 140
C     IF (PMF(KX,KZ).GT.1.E1M) SP(KX,KZ)=0. CRS 150
C     IF (PMF(KX,KZ).EQ.0.) SP(KX,KZ)=0. CRS 160
102  CONTINUE CRS 170
C
C FIND MAX AND MIN CRS 180
C
C DO 104 J0=1,NC CRS 190
C   DO 103 JP=1,ND CRS 200
103   PP(JP)=SP(J0,JP) CRS 210
104   CALL MAPA (E,G,PP,1,ND,HI,HH,VL,VH,X,Y,TI,1) CRS 220
C
C PLOT OF DATA CRS 230
C
C CALL MAPA (1,PXP,PYP,1,25,HL,HH,VL,VH,X,Y,TI,1) CRS 240
C CALL MAPM (1,PXP,PYP,1,25,ML,HH,VL,VH,X,Y,TE,1) CRS 250
C DO 112 IA=1,NC CRS 260
C   DO 105 IY=1,ND CRS 270
105   PR(IA)=SP(IA,IY) CRS 280
C   CALL >INTFP (G,PP,PXP,PYP,ND,25+3) CRS 290
C   XX=PNO(IY) CRS 300
C

```

```

      WRITE (6,113) XX
      WRITE (6,114) X(1),H(1)
      DO 106 IX=1,25
106   WRITE (6,115) PXP(IX),PYP(IX)
      WRITE (6,116) (PNE(IA,II),II=1,ND)
      WRITE (8,117) (G(IX)*PP(IX),IX=1,ND)

C     PLOT OF UTILIZATION VERSUS DISCHARGE POWER
C
      IF (IK.EQ.4.OR.IK.EQ.13) GO TO 107
      GO TO 111
107   IF (IK.EQ.13) GO TO 109
      DO 108 L=1,25
108   UTL(IA,L)=PYP(L)
      GO TO 111
109   DO 110 L=1,25
110   PD(IA,L)=PYP(L)
111   CONTINUE
      CALL MAPM (2,PXP,PYP,1,25,HL,HH,VL,VH,X,H,Z,1)
112 CALL MAPA (2,PXP,PYP,1,25,HL,HH,VL,VH,X,H,Z,1)
      CALL MAPA (4,PXP,PYP,1,25,HL,HH,VL,VH,X,H,Z,1)
      CALL MAPM (4,PXP,PYP,1,25,HL,HH,VL,VH,X,H,Z,1)
      RETURN

C
113 FORMAT (//,20X,13HPICKED VALUE=+2X,E10.3,4HMILLIAMPS)
114 FORMAT (/,10X,A10,20X,A10)
115 FORMAT (12X,F4.3,18X,F11.4,10X,E11.4)
116 FORMAT (/,5X,10HFLEC,DEFS.,8(2X,F10.3))
117 FORMAT (8F10.3)

C     END

      SUBROUTINE XINTERP (X,Y,XI,YI,NIN,NOUT,INTERP)
C
C     THIS SUBROUTINE RETURNS -NOUT- POINTS WHICH ARE INTERPOLATED TO
C     THE -INTERP- DEGREE FROM -X,Y-
C
      DIMENSION X(NIN), Y(NIN), XI(NOUT), YI(NOUT)
      DX=(X(NIN)-X(1))/FLAGT(NOUT-1)
      XX=X(1)
      DO 101 I=1,NOUT
         XI(I)=XX
         CALL AITKEN (X,Y,NIN,INTERP,XX,YY)
         IF (YY.LT.0.) YY=0.
         YI(I)=YY
101   XX=XX+DX
      RETURN

C     END

      SUBROUTINE YTNTEG (SIGMA,SIGNRG,PROP,SUM,PRSUM)
C
C     EVALUATION OF REACTION RATE
C
      COMMON /A/ NP,NM,T,PRINRG
      DIMENSION SIGMA(2+21), SIGNRG(2+21), SX(21), SE(21)
      REAL NP,NM

C     PRIMARY ELECTRONS
C
      DO 101 I=1,21
         SX(I)=SIGMA(1+I)
101   SE(I)=SIGMA(1+I)
      CALL AITKEN (SE,SX,21,2,PRINRG,RX)
      PRSUM=NP*PROB*RX
C

```

```

C      MAXWELLIAN ELECTRONS                               NTG  170
C
C      DO 102 I=1,21                                     NTG  180
C          SX(I)=SIGMA(2,I)                             NTG  190
C 102  SF(I)=SIGNRG(2,I)                               NTG  200
C      CALL AITKEN (SF,SX,21,2,T,TR)                   NTG  210
C      TSUM=PROP*NM*TR                                NTG  220
C      SUM=TSUM+PSUM                                 NTG  230
C      PRSUM=PSUM/SUM                                NTG  240
C      RETURN                                         NTG  250
C
C      END                                              NTG  260
C
C      SUBROUTINE SUMIT (SIG,SGF,N,PROP,TSUM,SUMS,PRSUMS)    SUM   10
C
C      TRANSFER ROUTINE FOR EXCITED STATES               SUM   20
C
C      COMMON /A/ NP,NM,TEMP,PRINRG                      SUM   30
C      DIMENSION SIG(N,2,21), SGE(N,2,21), PROP(N), SUMS(N), PRSUMS(N), SSUM  60
C 1X(2,25), SF(2,25)                                SUM   70
C      REAL NP,NM                                       SUM   80
C
C      CALCULATES THE SUM OF INTERVALS                  SUM   90
C
C      TSUM=0.                                         SUM  100
C      DO 102 I=1,N                                     SUM  110
C          DO 101 J=1,2                                SUM  120
C              DO 101 K=1,21                            SUM  130
C                  SX(J,K)=SIG(I,J,K)                 SUM  140
C 101      SF(J,K)=SGE(I,J,K)                         SUM  150
C      CALL YINTEG (SX,SE,PROP(I),SUMS(I),PRSUMS(I))    SUM  160
C 102  TSUM=TSUM+SUMS(I)                           SUM  170
C      RETURN                                         SUM  180
C
C      END                                              SUM  190
C
C      SUBROUTINE AITKEN (X,Y,N,K,XR,YR)                AIT   10
C
C      ***** AITKEN INTERPOLATION SUBROUTINE *****        AIT   20
C
C      CALLING SEQUENCE...                               AIT   30
C      CALL AITKEN(X,Y,N,K,XR,YR)                      AIT   40
C
C      X IS A ONE DIMENSIONAL ARRAY OF INDEPENDENT       AIT   50
C      VARIABLE (INCREASING OR DECREASING)               AIT   60
C      Y IS A ONE DIMENSIONAL ARRAY OF DEPENDENT        AIT   70
C      VARIABLE                                         AIT   80
C      N IS NO. OF X,Y PAIRS                           AIT   90
C      K IS DEGREE OF INTERPOLATING POLYNOMIAL (MAX = 10 ) AIT  100
C      XR IS INDEP. VARIABLE ARGUMENT                 AIT  110
C      YR IS INTERPOLATED RESULT                      AIT  120
C
C      ***** TYPE, DIMENSION AND LABELED COMMON STATEMENTS *****
C
C      TYPE, DIMENSION AND LABELED COMMON STATEMENTS      AIT  130
C
C      DIMENSION X(N), Y(N), XX(11), YY(11)             AIT  140
C      K1=K+1                                           AIT  150
C      IF (X(N)-X(1)) 110,101,101                     AIT  160
C 101  IF (XR-X(1)) 102,102,103                     AIT  170
C 102  LL=0                                           AIT  180
C      GO TO 119                                         AIT  190
C
C 103  IF (X(N)-XR) 104,104,105                     AIT  200
C 104  LL=N-K1                                         AIT  210
C      GO TO 119                                         AIT  220

```

```

C   105 LL=1          AIT 310
    LU=N          AIT 320
    IF (LU-LL-1) 117,117,107  AIT 330
    106 IF (LU-LL-1) 117,117,107  AIT 340
    107 LI=(LL+LU)/2          AIT 350
      IF (X(LI)-XB) 108,108,109  AIT 360
    108 LL=LI          AIT 370
      GO TO 104          AIT 380
C   109 LU=LI          AIT 390
      GO TO 106          AIT 400
C   110 IF (XB-X(I)) 111,102,102  AIT 410
    111 IF (X(N)-XB) 112,104,104  AIT 420
    112 LL=1          AIT 430
      LU=N          AIT 440
    113 IF (LU-LL-1) 117,117,114  AIT 450
    114 LI=(LL+LU)/2          AIT 460
      IF (X(LI)-XB) 115,116,116  AIT 470-
    115 LU=LI          AIT 480
      GO TO 113          AIT 490
C   116 LL=LI          AIT 500
      GO TO 113          AIT 510
C   117 LL=LL-(K1+1)/2          AIT 520
      IF (LL) 102,114,118          AIT 530
    118 IF (LL+K1-N) 119,119,104          AIT 540
    119 DO 120 I=1,K1          AIT 550
      I1=LL+I          AIT 560
      XX(I)=X(I1)-XB          AIT 570
    120 YY(J)=Y(I1)          AIT 580
      DO 121 I=1,K          AIT 590
      DO 121 J=I,K          AIT 600
        IF (XX(J+1).EQ.XX(I)) GO TO 122          AIT 610
    121 YY(J+1)=(1./(XX(J+1)-XX(I)))*(YY(I)*XX(J+1)-YY(J+1)*XX(I))          AIT 620
      YY=YY(K1)          AIT 630
      RETURN          AIT 640
    122 WRITE (6,123) (X(I),I=1,N)          AIT 650
      WRITE (6,123) (Y(I),I=1,N)          AIT 660
      WRITE (6,124)          AIT 670
      A=1./(XX(J+1)-XX(I))          AIT 680
      CCC=3.*A          AIT 690
      RETURN          AIT 700
C   123 FORMAT (10(2X,F10.3))          AIT 710
    124 FORMAT (10X,17#TROUBLE IN AITKEN)          AIT 720
C   END          AIT 730
&   5.0000 0.          6.0000 0.          7.0000 0.          MG-MG+          1
    8.0000 0.          9.0000 0.          10.0000 0.          MG-MG+          2
    11.0000 .624E-14    12.0000 .164E-13    14.0000 .339E-13HG-HG+          3
    16.0000 .505E-13    18.0000 .573E-13    20.0000 .837E-13HG-HG+          4
    23.5000 .111E-12    27.0000 .136E-12    30.0000 .153E-12HG-HG+          5
    33.5000 .172E-12    37.0000 .184E-12    40.0000 .198E-12HG-HG+          6
    42.0000 .205E-12    44.0000 .211E-12    46.0000 .230E-12HG-HG+          7
    3.0000 .225E-14    4.0000 .533E-14    4.3000 .742E-14HG-HG+          1
    4.7000 .103E-13    5.0000 .121E-13    5.1000 .141E-13HG-HG+          2
    5.7000 .161E-13    6.0000 .141E-13    6.3000 .214E-13HG-HG+          3
    6.7000 .244E-13    7.0000 .258E-13    7.5000 .308E-13HG-HG+          4
    8.0000 .348E-13    8.5000 .383E-13    9.0000 .429E-13HG-HG+          5
    9.5000 .469E-13    10.0000 .504E-13    10.5000 .549E-13HG-HG+          6
    11.0000 .589E-13    12.0000 .666E-13    13.0000 .740E-13HG-HG+          7
    5.0000 0.          6.0000 0.          7.0000 0.          HG-HG++          1
    8.0000 0.          9.0000 0.          10.0000 0.          HG-HG++          2

```

11.0000	0.	12.0000	0.	14.0000	0.	HG-HG++	-	3
16.0000	0.	18.0000	0.	20.0000	0.	HG-HG++	-	4
23.5000	0.	27.0000	0.	30.0000	.617E-15HG-HG++	-	5	
33.5000	.190E-14	.370000	.306E-14	.40.0000	.434F-14HG-HG++	-	6	
42.0000	.536E-14	.44.0000	.648E-14	.50.0000	.103F-13HG-HG++	-	7	
5.0000	.322E-18	.4.0000	.429E-17	.4.3000	.743F-17HG-HG++	-	1	
4.7000	.139E-16	.5.0000	.210E-16	.5.3000	.304F-16HG-HG++	-	2	
5.7000	.470E-16	.6.0000	.629E-16	.6.3000	.522F-16HG-HG++	-	3	
6.7000	.114E-15	.7.0000	.142E-15	.7.5000	.197F-15HG-HG++	-	4	
8.0000	.265F-15	.8.5000	.346E-15	.9.0000	.434F-15HG-HG++	-	5	
9.5000	.546F-15	.10.0000	.665E-15	.10.5000	.797F-15HG-HG++	-	6	
11.0000	.942E-15	.12.0000	.127E-14	.13.0000	.164F-14HG-HG++	-	7	
5.	-3. E-30	7.	-2.5 E-30	8.5	-2. F-30HG+ - HG++	-	1	
10.	-1.5 E-30	12.	-1.25E-30	14.	-1. F-30HG+ - HG++	-	2	
16.	-.5 F-30	18.6	0. E-30	19.25	.162 F-13HG+ - HG++	-	3	
20.	.443 E-13	20.5	.47 E-13	22.	.529 F-13HG+ - HG++	-	4	
25.	.657 F-13	27.5	.765 E-13	30.	.854 F-13HG+ - HG++	-	5	
33.	.941 F-13	37.	.1.02 E-13	40.	.1.1 E-13HG+ - HG++	-	6	
42.	1.15 E-13	46.	.1.24 E-13	50.	.1.33 F-13HG+ - HG++	-	7	
3.0000	.267F-15	4.0000	.127E-14	4.3000	.177F-14HG+ - HG++	-	1	
4.7000	.257E-14	5.0000	.327E-14	5.3000	.405E-14HG+ - HG++	-	2	
5.7000	.521E-14	6.0000	.516E-14	6.3000	.717F-14HG+ - HG++	-	3	
6.7000	.860E-14	7.0000	.973E-14	7.5000	.117E-13HG+ - HG++	-	4	
8.0000	.134E-13	8.5000	.159E-13	9.0000	.181F-13HG+ - HG++	-	5	
9.5000	.203F-13	10.0000	.226E-13	10.5000	.249F-13HG+ - HG++	-	6	
11.0000	.272E-13	12.0000	.318E-13	13.0000	.364F-13HG+ - HG++	-	7	
5.0000	.988F-14	6.0000	.121E-13	7.0000	.107F-13HG-HGM 3P0	1		
8.0000	.907F-14	9.0000	.744F-14	10.0000	.576F-14HG-HGM 3P0	2		
11.0000	.441E-14	12.0000	.333E-14	14.0000	.228F-14HG-HGM 3P0	3		
16.0000	.191E-14	18.0000	.123E-14	20.0000	.103F-14HG-HGM 3P0	4		
23.5000	.827F-15	27.0000	.720F-15	30.0000	.579F-15HG-HGM 3P0	5		
33.5000	.423E-15	37.0000	.286E-15	40.0000	.18HF-14HG-HGM 3P0	6		
42.0000	0.	44.0000	0.	50.0000	0.	HG-HGM 3P0	7	
3.0000	.319F-14	4.0000	.378E-14	4.3000	.387F-14HG-HGM 3P0	1		
4.7000	.395E-14	5.0000	.348E-14	5.3000	.394F-14HG-HGM 3P0	2		
5.7000	.393E-14	6.0000	.346E-14	6.3000	.343F-14HG-HGM 3P0	3		
6.7000	.388F-14	7.0000	.384E-14	7.5000	.376E-14HG-HGM 3P0	4		
8.0000	.367F-14	8.5000	.358E-14	9.0000	.348E-14HG-HGM 3P0	5		
9.5000	.339F-14	10.0000	.330E-14	10.5000	.321F-14HG-HGM 3P0	6		
11.0000	.312E-14	12.0000	.294E-14	13.0000	.278F-14HG-HGM 3P0	7		
5.0000	0.	6.0000	.437E-13	7.0000	.482F-13HG-HGM 3P2	1		
8.0000	.404F-13	9.0000	.329E-13	10.0000	.260F-13HG-HGM 3P2	2		
11.0000	.212F-13	12.0000	.185E-13	14.0000	.136F-13HG-HGM 3P2	3		
16.0000	.105F-13	18.0000	.799F-14	20.0000	.655F-14HG-HGM 3P2	4		
23.5000	.433F-14	27.0000	.312E-14	30.0000	.227F-14HG-HGM 3P2	5		
33.5000	.168F-14	37.0000	.144E-14	40.0000	.131F-14HG-HGM 3P2	6		
42.0000	.113F-14	44.0000	.416F-15	50.0000	.365F-17HG-HGM 3P2	7		
3.0000	.963F-14	4.0000	.125F-13	4.3000	.130F-13HG-HGM 3P2	1		
4.7000	.135F-13	5.0000	.138E-13	5.3000	.140F-13HG-HGM 3P2	2		
5.7000	.142E-13	6.0000	.143E-13	6.3000	.143E-13HG-HGM 3P2	3		
6.7000	.147F-13	7.0000	.142F-13	7.5000	.141F-13HG-HGM 3P2	4		
8.0000	.139F-13	8.5000	.137F-13	9.0000	.134F-13HG-HGM 3P2	5		
9.5000	.132F-13	10.0000	.124F-13	10.5000	.126E-13HG-HGM 3P2	6		
11.0000	.123F-13	12.0000	.118E-13	13.0000	.112F-13HG-HGM 3P2	7		
5.0000	.948F-14	6.0000	.761E-14	7.0000	.462F-14HG-HGR 3P1	1		
8.0000	.410F-14	9.0000	.624E-14	10.0000	.714F-14HG-HGR 3P1	2		
11.0000	.708F-14	12.0000	.504E-14	14.0000	.628F-14HG-HGR 3P1	3		
16.0000	.640F-14	18.0000	.641E-14	20.0000	.633F-14HG-HGR 3P1	4		
23.5000	.595F-14	27.0000	.527E-14	30.0000	.444F-14HG-HGR 3P1	5		
33.5000	.319F-14	37.0000	.161F-14	40.0000	0.	HG-HGR 3P1	6	
42.0000	0.	44.0000	0.	50.0000	0.	HG-HGR 3P1	7	
1.0000	.234F-14	4.0000	.315E-14	4.3000	.334F-14HG-HGR 3P1	1		
4.7000	.356F-14	5.0000	.371E-14	5.3000	.384F-14HG-HGR 3P1	2		
5.7000	.208F-14	6.0000	.408E-14	6.3000	.416F-14HG-HGR 3P1	3		
6.7000	.426F-14	7.0000	.432E-14	7.5000	.434F-14HG-HGR 3P1	4		
8.0000	.445F-14	8.5000	.443E-14	9.0000	.451F-14HG-HGR 3P1	5		

9.5000	.452F-14	10.0000	.451E-14	10.5000	.450E-14HG-HGR	3P1	6
11.0000	.448F-14	12.0000	.441E-14	13.0000	.433F-14HG-HGR	3P1	7
5.0000	0.	6.0000	0.	7.0000	.132E-13HG-HGR	1P1	1
8.0000	.349F-13	9.0000	.579F-13	10.0000	.818F-13HG-HGR	1P1	2
11.0000	.106E-12	12.0000	.130E-12	14.0000	.152F-12HG-HGR	1P1	3
16.0000	.179E-12	18.0000	.189E-12	20.0000	.194F-12HG-HGR	1P1	4
23.5000	.209F-12	27.0000	.215F-12	30.0000	.220F-12HG-HGR	1P1	5
33.5000	.223F-12	37.0000	.224E-12	40.0000	.224F-12HG-HGR	1P1	6
42.0000	.224F-12	44.0000	.224E-12	50.0000	.222F-12HG-HGR	1P1	7
3.0000	.166F-13	4.0000	.323E-13	4.3000	.372E-13HG-HGR	1P1	1
4.7000	.437F-13	5.0000	.485F-13	5.3000	.532F-13HG-HGR	1P1	2
5.7000	.594E-13	6.0000	.638E-13	6.3000	.682F-13HG-HGR	1P1	3
6.7000	.737F-13	7.0000	.777E-13	7.5000	.841E-13HG-HGR	1P1	4
8.0000	.901E-13	8.5000	.957E-13	9.0000	.101F-12HG-HGR	1P1	5
9.5000	.106F-12	10.0000	.111E-12	10.5000	.115F-12HG-HGR	1P1	6
11.0000	.119F-12	12.0000	.127E-12	13.0000	.133F-12HG-HGR	1P1	7
5.0000	0.	6.0000	.451E-15	7.0000	.865F-14HG-M-HG+3P0	1	
8.0000	.233F-13	9.0000	.355F-13	10.0000	.477F-13HGGM-HG+3P0	2	
11.0000	.590F-13	12.0000	.701E-13	14.0000	.916F-13HGGM-HG+3P0	3	
16.0000	.110F-12	18.0000	.130E-12	20.0000	.157E-12HGGM-HG+3P0	4	
23.5000	.205F-12	27.0000	.247E-12	30.0000	.278F-12HGGM-HG+3P0	5	
33.5000	.304F-12	37.0000	.335E-12	40.0000	.354F-12HGGM-HG+3P0	6	
42.0000	.365F-12	44.0000	.376E-12	50.0000	.400F-12HGGM-HG+3P0	7	
3.0000	.103E-13	4.0000	.210E-13	4.3000	.247F-13HGGM-HG+3P0	1	
4.7000	.294E-13	5.0000	.338E-13	5.3000	.378F-13HGGM-HG+3P0	2	
5.7000	.433F-13	6.0000	.476E-13	6.3000	.518E-13HGGM-HG+3P0	3	
6.7000	.575E-13	7.0000	.613E-13	7.5000	.690F-13HGGM-HG+3P0	4	
8.0000	.762F-13	8.5000	.834E-13	9.0000	.904F-13HGGM-HG+3P0	5	
9.5000	.974E-13	10.0000	.104E-12	10.5000	.111F-12HGGM-HG+3P0	6	
11.0000	.114F-12	12.0000	.131E-12	13.0000	.143F-12HGGM-HG+3P0	7	
5.0000	.682F-15	6.0000	.958F-14	7.0000	.312F-13HGGM-HG+3P2	1	
8.0000	.484F-13	9.0000	.652F-13	10.0000	.798F-13HGGM-HG+3P2	2	
11.0000	.929F-13	12.0000	.106E-12	14.0000	.129F-12HGGM-HG+3P2	3	
16.0000	.144F-12	18.0000	.164E-12	20.0000	.147E-12HGGM-HG+3P2	4	
23.5000	.244F-12	27.0000	.245E-12	30.0000	.316F-12HGGM-HG+3P2	5	
33.5000	.346F-12	37.0000	.371E-12	40.0000	.390F-12HGGM-HG+3P2	6	
42.0000	.400F-12	44.0000	.410E-12	50.0000	.433F-12HGGM-HG+3P2	7	
3.0000	.174F-13	4.0000	.327E-13	4.3000	.375F-13HGGM-HG+3P2	1	
4.7000	.442F-13	5.0000	.492E-13	5.3000	.542F-13HGGM-HG+3P2	2	
5.7000	.610E-13	6.0000	.661E-13	6.3000	.711F-13HGGM-HG+3P2	3	
6.7000	.774E-13	7.0000	.828E-13	7.5000	.911F-13HGGM-HG+3P2	4	
8.0000	.992F-13	8.5000	.107E-12	9.0000	.115F-12HGGM-HG+3P2	5	
9.5000	.123F-12	10.0000	.130E-12	10.5000	.138F-12HGGM-HG+3P2	6	
11.0000	.145F-12	12.0000	.159E-12	13.0000	.172F-12HGGM-HG+3P2	7	
5.0000	0.	6.0000	0.	7.0000	0.	HGM+	HG++5
8.0000	0.	9.0000	0.	10.0000	0.	HGM+	HG++5
11.0000	0.	12.0000	0.	14.0000	0.	HGM+	HG++5
16.0000	0.	14.0000	0.	20.0000	.625F-15HGMM	HG++5	4
23.5000	.722F-14	27.0000	.238E-13	30.0000	.396E-13HGMM	HG++5	5
33.5000	.576E-13	37.0000	.744E-13	40.0000	.877E-13HGMM	HG++5	6
42.0000	.454F-13	44.0000	.104E-12	45.0000	.124E-12HGMM	HG++5	7
3.0000	.379E-15	4.0000	.261E-15	4.3000	.347E-15HGMM	HG++5	1
4.7000	.642E-15	5.0000	.379E-15	5.3000	.116E-14HGMM	HG++5	2
5.7000	.152E-14	6.0000	.202E-14	6.3000	.247E-14HGMM	HG++5	3
6.7000	.319E-14	7.0000	.372E-14	7.5000	.477E-14HGMM	HG++5	4
8.0000	.594E-14	8.5000	.722E-14	9.0000	.360F-14HGMM	HG++5	5
9.5000	.101E-13	10.0000	.116E-13	10.5000	.133E-13HGMM	HG++5	6
11.0000	.149E-13	12.0000	.183E-13	12.5000	.221E-13HGMM	HG++5	7
5.0000	0.	6.0000	0.	7.0000	0.	HGM+-	HG++3
8.0000	0.	9.0000	0.	10.0000	0.	HGM+-	HG++3
11.0000	0.	12.0000	0.	14.0000	0.	HGM+-	HG++3
16.0000	0.	18.0000	0.	20.0000	.625E-15HGMM	HG++3	4
23.5000	.722F-14	27.0000	.239E-13	29.0000	.395E-13HGMM	HG++3	5
33.5000	.576E-13	37.0000	.745E-13	40.0000	.377E-13HGMM	HG++3	6
42.0000	.454E-13	44.0000	.105E-12	45.0000	.126E-12HGMM	HG++3	7
3.0000	.379E-15	.431E-15	.431E-15	.431E-15	.337E-15HGMM	HG++3	1

4.7000	.642F-15	5.0000	.874F-15	5.3000	.116F-14HGM+-HG++3	2
5.7000	.162F-14	5.0000	.202F-14	6.3000	.247F-14HGM+-HG++3	3
6.7000	.315F-14	7.0000	.372F-14	7.5000	.477F-14HGM+-HG++3	4
8.0000	.594F-14	8.5000	.722F-14	9.0000	.860F-14HGM+-HG++3	5
9.5000	.101F-13	10.0000	.116F-13	10.5000	.133F-13HGM+-HG++3	6
11.0000	.149F-13	12.0000	.185F-13	13.0000	.221F-13HGM+-HG++3	7
5.0000	0.	6.0000	.221F-14	7.0000	.129F-13HGR-HG+3P1	1
8.0000	.289F-13	9.0000	.423F-13	10.0000	.553F-13HGR-HG+3P1	2
11.0000	.670F-13	12.0000	.787F-13	14.0000	.101F-12HGR-HG+3P1	3
16.0000	.119F-12	18.0000	.140F-12	20.0000	.167F-12HGR-HG+3P1	4
23.5000	.214F-12	27.0000	.256F-12	30.0000	.288F-12HGR-HG+3P1	5
33.5000	.314F-12	37.0000	.344F-12	40.0000	.363F-12HGR-HG+3P1	6
42.0000	.374F-12	44.0000	.384F-12	50.0000	.409F-12HGR-HG+3P1	7
3.0000	.119F-13	4.0000	.237F-13	4.3000	.276F-13HGR-HG+3P1	1
4.7000	.331F-13	5.0000	.373F-13	5.3000	.416F-13HGR-HG+3P1	2
5.7000	.475F-13	6.0000	.519F-13	6.3000	.563F-13HGR-HG+3P1	3
6.7000	.623E-13	7.0000	.668F-13	7.5000	.743F-13HGR-HG+3P1	4
8.0000	.817E-13	8.5000	.890F-13	9.0000	.963F-13HGR-HG+3P1	5
9.5000	.103F-12	10.0000	.111F-12	10.5000	.117F-12HGR-HG+3P1	6
11.0000	.124F-12	12.0000	.137F-12	13.0000	.150F-12HGR-HG+3P1	7
5.0000	0.	6.0000	0.	7.0000	.743F-15HGR-HG+1P1	1
8.0000	.628F-14	9.0000	.161F-13	10.0000	.246F-13HGR-HG+1P1	2
11.0000	.338F-13	12.0000	.435F-13	14.0000	.625F-13HGR-HG+1P1	3
16.0000	.793F-13	18.0000	.984F-13	20.0000	.126F-12HGR-HG+1P1	4
23.5000	.173F-12	27.0000	.215F-12	30.0000	.247F-12HGR-HG+1P1	5
33.5000	.279F-12	37.0000	.305E-12	40.0000	.325E-12HGR-HG+1P1	6
42.0000	.336F-12	44.0000	.347F-12	50.0000	.372F-12HGR-HG+1P1	7
3.0000	.585F-14	4.0000	.134F-13	4.3000	.162F-13HGR-HG+1P1	1
4.7000	.201F-13	5.0000	.233F-13	5.3000	.265F-13HGR-HG+1P1	2
5.7000	.311F-13	6.0000	.346F-13	6.3000	.382F-13HGR-HG+1P1	3
6.7000	.431F-13	7.0000	.468F-13	7.5000	.531F-13HGR-HG+1P1	4
8.0000	.595F-13	8.5000	.659F-13	9.0000	.722F-13HGR-HG+1P1	5
9.5000	.788F-13	10.0000	.849F-13	10.5000	.912F-13HGR-HG+1P1	6
11.0000	.974F-13	12.0000	.109F-12	13.0000	.121F-12HGR-HG+1P1	7
5.0000	.174F-13	6.0000	.188F-13	7.0000	.200F-13HGR-HGM+5	1
8.0000	.210F-13	9.0000	.219F-13	10.0000	.227F-13HGR-HGM+5	2
11.0000	.235F-13	12.0000	.241F-13	14.0000	.250F-13HGR-HGM+5	3
16.0000	.216F-13	14.0000	.190F-13	20.0000	.168F-13HGR-HGM+5	4
23.5000	.137F-13	27.0000	.113F-13	30.0000	.967F-14HGR-HGM+5	5
33.5000	.817E-14	37.0000	.647F-14	40.0000	.613F-14HGR-HGM+5	6
42.0000	.464F-14	44.0000	.521F-14	50.0000	.416F-14HGR-HGM+5	7
3.0000	.806F-14	4.0000	.108F-13	4.3000	.114F-13HGR-HGM+5	1
4.7000	.122F-13	5.0000	.176F-13	5.3000	.130F-13HGR-HGM+5	2
5.7000	.135F-13	6.0000	.138F-13	6.3000	.140F-13HGR-HGM+5	3
6.7000	.143F-13	7.0000	.144F-13	7.5000	.146F-13HGR-HGM+5	4
8.0000	.147F-13	8.5000	.148F-13	9.0000	.148F-13HGR-HGM+5	5
9.5000	.148F-13	10.0000	.148F-13	10.5000	.147F-13HGR-HGM+5	6
11.0000	.146E-13	12.0000	.144E-13	13.0000	.141F-13HGR-HGM+5	7
5.0000	0.	6.0000	0.	7.0000	.154F-13HGR-HGM+3	1
8.0000	.164F-13	9.0000	.173F-13	10.0000	.181F-13HGR-HGM+3	2
11.0000	.198F-13	12.0000	.194F-13	14.0000	.202F-13HGR-HGM+3	3
16.0000	.180F-13	18.0000	.157F-13	20.0000	.143F-13HGR-HGM+3	4
23.5000	.112F-13	27.0000	.922F-14	30.0000	.789F-14HGR-HGM+3	5
33.5000	.664F-14	37.0000	.565F-14	40.0000	.422F-14HGR-HGM+3	6
42.0000	.455F-14	44.0000	.421F-14	50.0000	.375F-14HGR-HGM+3	7
3.0000	.613F-14	4.0000	.633F-14	4.3000	.690F-14HGR-HGM+3	1
4.7000	.754F-14	5.0000	.777F-14	5.3000	.753F-14HGR-HGM+3	2
5.7000	.882F-14	6.0000	.911F-14	6.3000	.937F-14HGR-HGM+3	3
6.7000	.967F-14	7.0000	.963F-14	7.5000	.101F-13HGR-HGM+3	4
8.0000	.103F-13	8.5000	.103F-13	9.0000	.106F-13HGR-HGM+3	5
9.5000	.105F-13	10.0000	.107F-13	10.5000	.107F-13HGR-HGM+3	6
11.0000	.107F-13	12.0000	.115F-13	13.0000	.109F-13HGR-HGM+3	7
1. 1	6. 1					
1.	1.	400.	6.1	6.1		
.014	4.2	27.5	2.3	9.4	7.16	

APPENDIX B

The computer program "PROP" is listed below. It can be used to determine the values of the volume averaged plasma properties and the uniformity factors needed by the computer program "HG." The data needed to determine these quantities is obtained from a Langmuir probe survey of the discharge chamber in which the plasma properties are determined at many different locations within the chamber. This data is used to numerically evaluate Equations (10) to (15) and (21) yielding the volume averaged plasma properties and the uniformity factors. Comment cards are included in the computer program to indicate the purpose of each section. A CDC 6400 computer will use approximately thirty seconds of Central Processor time to evaluate five sets of data obtained from five Langmuir probe surveys.

```

PROGRAM PROB (INPUT,OUTPUT,TAPE5=INPUT,TAPE6=OUTPUT)      PRP  10
C
C THIS PROGRAM CALCULATES THE AVERAGE PROPERTIES          PRP  20
C PLS=RADIAL POSITION OF LANGMUIR PROBE POINTS (1-CENTERLINE) PRP  30
C POS=POS. OF DESIRED DATA POINTS IF NR .NE. 4            PRP  40
C POSZ=AXIAL POSITION OF LANGMUIR PROBE POSITIONS (1-UPSTREAM PNT.) PRP  50
C NT-NO. OF TRACES PER SET      NR-MU. OF RADIAL POINTS    PRP  60
C IFLAG=1 IF ONE WANTS TO PRODUCE A SET OF POINTS UPSTREAM PRP  70
C IFLAG=2 POINTS PRODUCED AT THE BAFFLE                  PRP  80
C DIS=DISTANCE FROM SCREEN TO POINT WHERE THE GENERATED SET IS TO PRP  90
C RF PLACED
C RCATH=CATHODE RADIUS                                     PRP 100
C ENP=LENGTH OF PRIMARY ELECTRON REGION AT CENTERLINE    PRP 110
C
C DIMENSION XNP(72), XNM(72), T(70), Z(70), V(50), ZI(21), R(21), F(PRP 120
C 121), TF(21), AA(5), RR(5), CC(5), DD(5), FE(5), FF(5), FND(11), POPRP 130
C 2S(5), W(11), POSZ(11), YT(11), YP(11), YM(11), YZ(11), POR(10), AAPPP 140
C 3A(10), VF(51)
C DIMENSION AT(70), AZ(70), ANP(70), ANM(70), A(11), B(11), C(11), DPRP 150
C 1(11), E(11), VT(11), PI,S(5)
C DATA AA,RR,CC,DD,EE/25*0.1
C DATA POS /0.,1.1,2.2,3.3*4./
C DATA PLS /0.,1.,2.,3.,3.5/
C
C INTEGRATED CROSS SECTIONS FOR + TO ++
C
C READ (5,129) (7I(I),F(I),I=1,21)                      PRP 240
C READ (5,129) (TF(I),G(I),I=1,21)                      PRP 250
C WRITE (6,133) (ZI(I),F(I),I=1,21)                      PRP 260
C WRITE (6,133) (TF(I),G(I),I=1,21)                      PRP 270
C PI=6.2832
101 READ (5,126) NR,NT,IFLAG,DIS,RCATH,ENP             PRP 280
  IF (EOF(5)) 125,102,125
102 ND=NT/NR
  NN=ND
  IF (IFLAG,NE.0) NN=ND+1
  READ (5,127) (POSZ(I),I=1,ND)
C
C RADIAL DISTANCE TO CRITICAL FIELD LINE                PRP 290
C
C READ (5,127) (FND(I),I=1,NN)                         PRP 300
C
C READ IN THE PROPERTIES                                PRP 310
C
C DO 103 I=1,NT                                         PRP 320
103 READ (5,130) T(I),Z(I),XNP(I),XNM(I)              PRP 330
  IF (NR,EO,4) GO TO 104
  IS=0
  DO 106 J=1,NT
    NND=I+NR-1
    DO 104 J=1,NND
      K=J+1-I
      YT(K)=T(J)
      YP(K)=XNP(J)
      YM(K)=XNM(J)
      YZ(K)=Z(J)
    DO 105 J=1,4
      L=J+IS
      CALL ATTFEN (PLS,YT,K,L,POS(L),AT(L))
      CALL ATTFEN (PLS,YP,K,L,POS(L),AMP(L))
      CALL ATTFEN (PLS,YM,K,L,POS(L),ANM(L))
104    CALL ATTFEN (PLS,YZ,K,L,POS(L),AZ(L))
105    IS=IS+4
  NT=NT*4/NR
  ND=NT/4

```

```

DC 107 J=1,NT          PRP 660
T(J)=AT(J)             PRP 670
Z(J)=AZ(J)             PRP 680
XNP(J)=ANP(J)          PRP 690
107 XNM(J)=ANM(J)      PRP 700
WHITE (6+130) (T(N)+Z(N)+XNP(N)+XNM(N),N=1,NT) PRP 710
108 IF (IFLAG,FQ,0) GO TO 114 PRP 720
C   CALCULATION OF THE EXTRA SET OF POINTS PRP 730
C
N=1                   PRP 740
DO 110 I=1,4           PRP 750
L=0                   PRP 760
DO 109 J=I,NT+4        PRP 770
L=I+1                 PRP 780
YT(L)=T(J)             PRP 790
YP(L)=XNP(J)           PRP 800
YM(L)=XNM(J)           PRP 810
109 YZ(L)=Z(J)          PRP 820
K=NT+I                 PRP 830
CALL ATTKEN (POSZ,YT,MD,N,DIS,AT(K)) PRP 840
K=NT+I                 PRP 850
CALL ATTKEN (POSZ,YT,MD,N,DIS,AT(K)) PRP 860
CALL ATTKEN (POSZ,YZ,MD,N,DIS,AZ(K)) PRP 870
CALL ATTKEN (POSZ,YP,MD,N,DIS,ANP(K)) PRP 880
CALL ATTKEN (POSZ,YM,MD,N,DIS,ANM(K)) PRP 890
IF (AT(K).LT.0.) AT(K)=0.0 PRP 900
IF (AZ(K).LT.0.) AZ(K)=0.0 PRP 910
IF (ANP(K).LT.0.) ANP(K)=0.0 PRP 920
IF (ANM(K).LT.0.) ANM(K)=0.0 PRP 930
WHITE (6+128) AT(K)+AZ(K)+ANP(K)+ANM(K) PRP 940
110 CONTINUE            PRP 950
C   RESHUFFLING OF POINTS PRP 960
C
ND=ND+1                PRP 970
NNN=ND-1                PRP 980
XX=END(ND)              PRP 990
DO 111 J=1,NNN           PRP 1000
J=ND+1-I                PRP 1010
END(J)=END(J-1)          PRP 1020
111 POSZ(J)=POSZ(J-1)    PRP 1030
END(1)=XX                PRP 1040
POSZ(1)=DIS               PRP 1050
NT=NT+4                  PRP 1060
ND=NT/4                  PRP 1070
DO 112 I=5,NT             PRP 1080
K=NT+5-I                 PRP 1090
J=K-4                   PRP 1100
T(K)=T(J)                 PRP 1110
Z(K)=Z(J)                 PRP 1120
XP(K)=XNP(J)              PRP 1130
112 XNM(K)=XNM(J)          PRP 1140
NTM=NT-3                  PRP 1150
DO 113 I=NTM,NT             PRP 1160
J=I-NTM+1                 PRP 1170
T(J)=AT(I)                 PRP 1180
Z(J)=AZ(I)                 PRP 1190
XP(I)=ANP(I)               PRP 1200
113 XNM(I)=ANM(I)          PRP 1210
C   START OF THE CALCULATIONS
C
114 DO 115 I=1,ND           PRP 1220
I=I+(I-1)+1               PRP 1230
I=I+4                     PRP 1240

```

```

C THIS PRODUCES AN ARRAY OF F(0) AT CONSTANT Z POINTS          PRP 1300
C                                                               PRP 1310
C                                                               PRP 1320
C                                                               PRP 1330
C DO 117 J=1,K          PRP 1340
C M=J+1                PRP 1350
C R=POE(M)*PI          PRP 1360
C CALL ATTKEN (TF+Z1*2+F(J)+G1)          PRP 1370
C CALL ATTKEN (Z1*F+Z1*2+Z(J)+G1)          PRP 1380
C XT=XNP(J)+XNM(J)          PRP 1390
C TF (XNM(J)+EQ,0.0) GO TO 115          PRP 1400
C TERM=1.0+XNP(J)/XNM(J)          PRP 1410
C GO TO 116          PRP 1420
C TERM=1.0          PRP 1430
115   VF(J)=C*VFT(T(J)*4.803E9*TERM)          PRP 1440
C A(Y)=XNP(J)*XT*F1*R          PRP 1450
C RR(M)=XT*R          PRP 1460
C CC(M)=XT*R*XNP(J)          PRP 1470
C DD(M)=XNM(J)*XT*R          PRP 1480
C FF(M)=XNM(J)*XT*R          PRP 1490
117   FF(M)=R          PRP 1500
C
C INTEGRATION OF F YIELDING G(Z)          PRP 1510
C
C M=4          PRP 1520
C NM=19          PRP 1530
C CALL INTK (POS+AA*NM,2+END(I)+H)          PRP 1540
C A(I)=H          PRP 1550
C IF (IFLAG,NE,1,0,1,NE+1) GO TO 118          PRP 1560
C CALL INTK (POS+AA*NM,2+RCATH+HM)          PRP 1570
C A(I)=A(I)+HM          PRP 1580
C 118   CALL INTK (POS+EE,M+NM,2+END(I)+H)          PRP 1590
C R(I)=R          PRP 1600
C IF (IFLAG,NE,1,0,1,NE+1) GO TO 119          PRP 1610
C CALL INTK (POS+EE,M+NM,2+RCATH+HM)          PRP 1620
C R(I)=R(I)+HM          PRP 1630
C 119   CALL INTK (POS+CC,M+NM,2+END(I)+H)          PRP 1640
C C(I)=H          PRP 1650
C IF (IFLAG,NE,1,0,1,NE+1) GO TO 120          PRP 1660
C CALL INTK (POS+CC,M+NM,2+RCATH+HM)          PRP 1670
C C(I)=C(I)+HM          PRP 1680
C 120   CALL INTK (POS+FF,M+NM,2+END(I)+H)          PRP 1690
C D(I)=H          PRP 1700
C IF (IFLAG,NE,1,0,1,NE+1) GO TO 121          PRP 1710
C CALL INTK (POS+FF,M+NM,2+RCATH+HM)          PRP 1720
C D(I)=D(I)+HM          PRP 1730
C 121   CALL INTK (POS+EE,M+NM,2+END(I)+H)          PRP 1740
C E(I)=H          PRP 1750
C IF (IFLAG,NE,1,0,1,NE+1) GO TO 122          PRP 1760
C CALL INTK (POS+EE,M+NM,2+RCATH+HM)          PRP 1770
C E(I)=E(I)+HM          PRP 1780
C 122   CALL INTK (POS+FF,M+NM,2+END(I)+H)          PRP 1790
C VT(I)=H          PRP 1800
C IF (IFLAG,NE,1,0,1,NE+1) GO TO 123          PRP 1810
C CALL INTK (POS+FF,M+NM,2+RCATH+HM)          PRP 1820
C VT(I)=VT(I)+HM          PRP 1830
C 123 CONTINUE          PRP 1840
C
C INTEGRATION OF A DIRECTION          PRP 1850
C
C M=NM          PRP 1860
C CALL ATTKEN (TF+Z1*2+F(J)+G1)          PRP 1870
C CALL ATTKEN (Z1*F+Z1*2+Z(J)+G1)          PRP 1880
C VA=VA+KA          PRP 1890
C CALL ATTKEN (TF+Z1*2+F(J)+G1)          PRP 1900
C CALL ATTKEN (Z1*F+Z1*2+Z(J)+G1)          PRP 1910

```



```

CALL XTINTERP (X,Y,A,P,NIN,NUSED,INT)          NTG    70
CALL GTEG (A,B,C,NUSED)                         NTG    80
CALL ATTEN (A,C,NUSED,EN,XP,YP)                 NTG    90
RETURN                                         NTG   100
NTG   110
NTG   120

C
END

SUBROUTINE AREA (XP, XNM, XKEE, RTH, DTY, NLEN, R, VE, VEA)      ARA    10
C
C THIS SUBROUTINE CALCULATES THE PLASMA NONUNIFORMITY FACTORS      ARA    20
C PRY-POINTS (Z) DEFINING PRIMARY FIELD LINE (FROM SCREEN GRID)      ARA    30
C PRR-POINTS (M) DEFINING PRIMARY FIELD LINE (FROM CENTER LINE)      ARA    40
C NPRL=NO. OF PRIMARY FIELD LINE POINTS                           ARA    50
C IFLAG=1 IF LOSSES ARE ALLOWED TO THE CATHODE POLE PIECE        ARA    60
C DI=DISTANCE TO BAFFLE FROM SCREEN                            ARA    70
C CZU=POINT WHERE PRIMARY FIELD LINE INTERSECTS CATHODE POLE PIECE ARA    80
C (IF IFLAG=1)                                                 ARA    90
C                                                 ARA   100
C                                                 ARA   110
C
C DIMENSION DTR(5), DTY(10), X11(11), X12(11), X13(11), X14(11), PPRARA 120
C 1(10), PRY(10), P(5), Z(5), XNP(51), XNM(51), Q(5), VE(51), V(5), VARA 130
C 2F1(11), VE2(11), VE3(11), VE4(11)                           ARA   140
C REAL I,I2
C NFLAG=0
C MFLAG=0
C READ (5,107) NPRL,IFLAG,DI,CZU
C CZD=DI
C READ (5,111) (PPR(I),PRY(I),I=1,NPRL)
C NLEN=N*4
C
C BEGIN CALCULATIONS
C SHUFFLE NO. DENSITIES INTO CORRECT ARRAYS
C
C DO 101 I=1,NPRL
C     J=I+1
C     K=I+2
C     L=I+3
C     M=I+4+1
C     VE1(M)=VE(I)
C     VE2(M)=VE(J)
C     VE3(M)=VE(K)
C     VE4(M)=VE(L)
C     X12(M)=XNP(J)+XNM(J)
C     X13(M)=XNP(K)+XNM(K)
C     X14(M)=XNP(L)+XNM(L)
C 101 X11(M)=XNP(I)+XNM(I)

C
C     WRITE (6,110) (X11(I)+I=1+NLEN)                          ARA   400
C     WRITE (6,110) (X12(I)+I=1+NLEN)                          ARA   410
C     WRITE (6,110) (X13(I)+I=1+NLEN)                          ARA   420
C     WRITE (6,110) (X14(I)+I=1+NLEN)                          ARA   430
C     AZ=0.
C     DY=DY*(NLEN)/AZ00.
C     AR=0.
C     AR=0.
C     YZ=0*Y/2.
C
C     WRITE (6,110) (X11(I)+I=1+NLEN)                          ARA   440
C     WRITE (6,110) (X12(I)+I=1+NLEN)                          ARA   450
C     WRITE (6,110) (X13(I)+I=1+NLEN)                          ARA   460
C     WRITE (6,110) (X14(I)+I=1+NLEN)                          ARA   470
C     ARA   480
C     ARA   490
C     ARA   500
C     ARA   510
C     ARA   520
C     ARA   530
C     ARA   540
C     ARA   550
C     ARA   560
C     ARA   570
C     ARA   580
C     ARA   590
C
C     WRITE (6,110) (X11(I)+I=1+NLEN)                          ARA   590
C     WRITE (6,110) (X12(I)+I=1+NLEN)                          ARA   600
C     WRITE (6,110) (X13(I)+I=1+NLEN)                          ARA   610
C     WRITE (6,110) (X14(I)+I=1+NLEN)                          ARA   620
C
C     CALL ATTEN (A,C,NUSED,EN,XP,YP)                           ARA   630

```

```

CALL AITKEN (PHY,PKH,NPHF,1,TP,DP)          ARA 600
CALL AITKEN (PHY,PKH,NPHF,1,YM,DM)          ARA 610
DX=DP-DM
N=1
IF (I.GT.224) N=1
CALL AITKEN (DTY,X11,NLN,N,YZ,P(1))        ARA 620
CALL AITKEN (DTY,X12,NLN,N,YZ,P(2))        ARA 630
CALL AITKEN (DTY,X13,NLN,N,YZ,P(3))        ARA 640
CALL AITKEN (DTY,X14,NLN,N,YZ,P(4))        ARA 650
CALL CHECK (P,4,MFLAG)                      ARA 660
J=4
P(5)=P(4)/5.
CALL AITKEN (DTY,VE1,NLN,N,YZ,V(1))        ARA 670
CALL AITKEN (DTY,VE2,NLN,N,YZ,V(2))        ARA 680
CALL AITKEN (DTY,VE3,NLN,N,YZ,V(3))        ARA 690
CALL AITKEN (DTY,VE4,NLN,N,YZ,V(4))        ARA 700
CALL CHECK (V,4,MFLAG)                      ARA 710
V(5)=V(4)/5.
CALL AITKEN (DTR,P,J,N,YP,XNE)              ARA 720
CALL AITKEN (DTR,V,J,M,XP,VEE)              ARA 730
YZ=YZ+DY
AR=AR+SQRT(DX**2+DY**2)*6.2832*XP
AZ=AZ+SQRT(DX**2+DY**2)*6.2832*XP*XNE**2*VEE
102 AN=AN+SQRT(DX**2+DY**2)*6.2832*XP*XNE*VEE
C SECTION FOR GRIDS
C
P(1)=6.2832*DTR(1)*X11(NLN)
P(2)=6.2832*DTR(2)*X12(NLN)
P(3)=6.2832*DTR(3)*X13(NLN)
P(4)=6.2832*DTR(4)*X14(NLN)
CALL CHECK (P,4,MFLAG)
P(5)=0.
V(1)=VE1(NLN)
V(2)=VE2(NLN)
V(3)=VE3(NLN)
V(4)=VE4(NLN)
V(5)=0.
DO 103 IK=1,5
103 Q(IK)=V(IK)*P(IK)
CALL QTFG (DTR,Q,Z,S)
WHITE (6,108) Z(S)
I1=Z(S)
AN=AN+Z(S)
DO 104 IK=2,5
104 Q(IK)=Q(IK)*P(IK)/(6.2832*DTR(IK))
CALL QTFG (DTR,Q,Z,S)
I2=Z(S)
AZ=AZ+Z(S)
Z(S)=Z(S)*2.2H28
WRITE (6,108) Z(S)
AR=AR+3.14159*DTR(S)**2
Q(S)=0.
C SECTION FOR RAFFLE
C
N=1
CALL AITKEN (DTY,X11,NLN,N,DI,P(1))
CALL AITKEN (DTY,X12,NLN,N,DI,P(2))
CALL AITKEN (DTY,X13,NLN,N,DI,P(3))
CALL AITKEN (DTY,X14,NLN,N,DI,P(4))
CALL CHECK (P,4,MFLAG)
CALL AITKEN (DTY,VE1,NLN,N,DI+V(1))
CALL AITKEN (DTY,VE2,NLN,N,DI+V(2))
CALL AITKEN (DTY,VE3,NLN,N,DI+V(3))
CALL AITKEN (DTY,VE4,NLN,N,DI+V(4))

```



```

107 FORMAT (2I5+4F10.4)                                ARA 1920
108 FORMAT (2X, 4HI (CM-1)=,F11.4)                      ARA 1930
109 FORMAT (2X, 40HNEGATIVE VELOCITY EXTRAPOLATION OCCURRED,I5, 7H TARA 1940
    TIMES)                                              ARA 1950
110 FORMAT (10X,R(F10.3+2X))                           ARA 1960
111 FORMAT (F10.5)                                     ARA 1970
112 FORMAT (3X, 13HAN (CM2/CH3)=,F11.4)                ARA 1980
113 FORMAT (3X, 4HAR (CM2)=,F11.4)                      ARA 1990
114 FORMAT (3X, 13HAZ (CM2/CH5)=,F11.4)                ARA 2000
115 FORMAT (2X, 3HF1=,F10.4+2X, 3HF2=,F10.4+2X, 13HI++/I+ FACTOR,F10A ARA 2010
    1.4)
116 FORMAT (2X, 34HNEGATIVE TENSITY EXTRAPOLATION OCCURRED,I5, 8H TARA 2020
    TIMES)                                              ARA 2030
C
C
      END                                                 ARA 2040
      SUBROUTINE CHECK (P,N,NFLAG)                         ARA 2050
      DIMENSION P(N)                                       ARA 2060
      DO 101 I=1,N
        IF (P(I).GE.+0.0) GO TO 101
        P(I)=0.0
        NFLAG=NFLAG+1
101  CONTINUE
      RETURN
C
      END
#

```